THE FLOW OF WATER IN SALT MARSH PEAT

by

WILLIAM KENSETT NUTTLE

B.S. University of Maryland, College Park
(1980)

Submitted to the Department of
Civil Engineering
in Partial fulfillment of the
Requirements of the Degree of

MASTER OF SCIENCE

at the

MASSACHUSETTS INSTITUTE OF TECHNOLOGY

June 1982

© Massachusetts Institute of Technology 1982

Signature of Author _____
Department of Civil Engineering
May 14, 1982

Certified by _____
Harold F. Hemond
Thesis Supervisor

Accepted by _____
Francois M. M. Morel
Chairman, Department Committee

MASSACHUSETTS INSTITUTE OF TECHNOLOGY

JUL 26 1982

LIBRARIES Archives

THE FLOW OF WATER IN SALT MARSH PEAT

by

WILLIAM KENSETT NUTTLE

Submitted to the Department of Civil Engineering
on May 14, 1982 in partial fulfillment of the
requirements for the Degree of Master of Science in
Civil Engineering

ABSTRACT

A study of water flow in salt marsh peat in the Great Sippewissett Marsh is presented. Observations of the subsurface flow regime take two forms: 1) direct observations of water fluxes and piezometric potentials, and 2) laboratory determination of the hydraulic properties of peat. A simple linear flow equation is derived from the basic principles of fluid flow in a saturated porous medium. Using this equation, some simple models of the flow patterns in the peat are obtained. The models are tested by using the laboratory derived parameters to predict ranges of responses for the observed processes, without calibration. The comparison is good. Therefore, the flow models provide a means of describing the flow patterns in the peat. The flow of water in salt marsh peat is modeled for three processes: infiltration due to surface flooding, tidal forcing, and the long-term water balance.

Thesis Supervisor: Dr. Harold F. Hemond

Title: Assistant Professor of Civil Engineering

ACKNOWLEDGEMENTS

Dr. Richard Codell of the Nuclear Regulatory Commission demonstrated interest and encouragement for my work there as a co-op student. He is responsible for my decision to pursue graduate studies at M.I.T., a pursuit which I have found very rewarding. For this I owe him a debt of gratitude.

Professors Harry Hemond and Keith Stolzenbach are more directly responsible for the work presented here. Harry served as my thesis advisor and Keith as my academic advisor. I acknowledge their support and encouragement.

Jayne Fifield and Roger Burke preceded me in these investigations. They are directly responsible for pioneering the field and laboratory techniques and collecting the bulk of the data that I have used. Undergraduates Edmond Ho, Mark Schaefer, and Phillip Soo provided invaluable assistance in the laboratory and with the data reduction. This document is in large a summary of the contributions of these people, and I can only hope that I have served them well.

I am indebted to Barbara Adams for the many hours spent in preparing the manuscript.

This study has been supported by a grant from NOAA, Department of Commerce, the Office of Sea Grant, Grant #04-7-158-44079.

CONTENTS

1.0 Introduction

The biogeochemistry of coastal salt marshes is a current topic of research. Much of the chemistry of interest takes place within the salt marsh peat deposits. In order to understand the biological and chemical processes that occur, the availability of materials from outside of the peat must be specified. Chemical substances enter and exit the peat dissolved in water. There are three different sources of water in the marsh: sea water, precipitation, and fresh groundwater; each with its own chemical characteristics. Investigators have inferred exchange rates with external material sources and patterns of internal circulation from observations of chemical properties of pore water (Gardner, 1973; Howarth and Teal, 1979; Lindberg and Harriss, 1973).

An objective analysis of the chemical and biological processes occurring in salt marsh peat requires the independent knowledge of flow patterns within the peat and exchanges across the peat boundaries. The determination of these flow patterns from the principles of fluid mechanics and by direct measurement has been the objective of a four-year study at M.I.T. Burke (1979) made measurements of the rate of infiltration by sea water flooding the Great Sippewissett Marsh near Falmouth, Massachusetts at high tide using a device described by Hemond and Burke (1981). Measurements of the exchange of water through the creek banks and creek bottoms were also made using a device described by Lee (1977). Fifield (1981) designed and carried out a coring program in the Sippewisset Marsh and the Ebbens Creek Marsh near

Gloucester, Massachusetts. Hydraulic conductivity of the peat was measured using both laboratory techniques and field procedures. Hemond and Fifield (1982) were able to demonstrate the importance of evapotranspiration to the water balance in the peat by numerically modeling the response of a column of peat to evapotranspiration and tidal forcing. The model results were compared to the dynamic response of an actual peat deposit observed with a recording piezometer described by Hemond (1982). This study presents the results of laboratory work to determine the compressibility of peat from the cores taken from the Sippewissett Marsh. With hydraulic conductivity and compressibility of peat known, the dynamic and steady state flow patterns in the peat can be modeled. A simple analytic approach to the flow modeling is pursued here and the results compare well with the field observations.

Previous efforts to investigate water circulation in salt marshes are few. Niedorada and April (1975) instrumented two Cape Cod marshes with piezometers and observed the progression of flow patterns through a tidal cycle. Their work focussed on the flow of water in an underlying fresh water aquifer, however, and revealed little of the flow regime within the peat. Howland (1976) observed the variations in piezometric readings in the peat of a West Coast salt marsh due to tidal forcing at the creek bank. A numerical model of water flow in the peat was used to try to estimate the geometry of the flow field and the hydraulic properties of the peat by fitting with the observed piezometer responses. The model formulation was based on the Dupuit-Forchheimer assumptions that 1) predominately horizontal flow takes

place only below the water table, and 2) storativity is the result of saturation and desaturation of the peat as the water table moves up and down.

Observations suggest that full saturation of the peat is frequently realized and may be a good first approximation to use in an analysis of water flow in peat. Hemond and Fifield (1982) used a saturated-unsaturated model in their one dimensional flow analysis and found that desaturation did not occur after four days of drying the peat by evapotranspiration. If full saturation is assumed then the storativity of the peat is due entirely to its compressibility. In this case the equation governing the flow of water in the peat takes the form of a diffusion equation in terms of the piezometric potential, and analytic solutions of the flow can be obtained for some simple boundary conditions.

Investigation into the flow of water in the peat of the Sippewissett Marsh has produced two independent data sets: 1) a set of field observations of fluxes at the peat boundaries and fluxes implied by observed distributions and variations in piezometric potential in the peat, and 2) a set of laboratory measurements of the hydraulic properties of peat. The measured hydraulic properties can be used in the context of a flow model to predict the field observations. If predicted values match the observed values then the flow field characteristics assumed in the model formulation or implied by the model are supported. This technique has been used by Hemond and Fifield (1982) to show the predominance of evapotranspiration among

the processes driving the vertical flow of water in peat far from the creek.

This study extends the modeling approach to the analysis of the infiltration process due to flooding of the marsh surface and the periodic exchange of water across the creek banks due to tidal forcing. Results of the analysis of infiltration are used to speculate on the spatial variation in the time averaged infiltration input at the peat surface. A horizontal water balance is then formulated using estimates of precipitation inputs and evapotranspiration demand. The water balance demonstrates the possible variation in flow patterns and flux magnitudes in the peat with distance from a creek. The variability in water fluxes in the marsh due to random variation of the hydraulic properties of peat is also addressed.

2.0 The Mechanics of a Saturated Porous Medium

Salt marsh peat is a highly organic soil deposited as the result of the availability of mineral sediments in coastal waters and the activities of salt marsh plants and animals. Peat found in the Great Sippewissett Marsh near Falmouth, Massachusetts, has an organic content that varies between a few per cent and over 50% of the dry weight. Peat deposits in salt marshes are found in the intertidal zone of embayments and protected coastal areas and are frequently flooded by high tides. Hydraulic conductivity of the peat in the Sippewissett Marsh ranges from 10^{-2} cm/s to 10^{-6} cm/s with the upper margin of peat being generally the least permeable. The water table is very close to the peat surface, and the capillary fringe may extend all the way up to the peat surface. Field observations in the Sippewissett Marsh suggest that the peat is fully saturated most of the time.

The conditions of full saturation of a water bearing deposit at the surface is unique to wetlands. Most approaches to modeling the flow of water in surface or phreatic aquifers assume that the soil is saturated only below the water table and that flow takes place only in the saturated zone. Some approaches account for the fact that capillary effects may cause the zone of saturation to extend somewhat above the water table. The storage of water in surface aquifers is assumed by standard models to be the result of saturation and desaturation of soil as the water table rises and falls. This assumption is embodied in the concept of specific yield, which Bear (1979) defines as "the volume of water per unit area of soil, drained from a soil column

extending from the water table to the ground surface, per unit lowering of the water table." When a soil is fully saturated it does not drain, in the conventional sense of the word, due to fluctuations in the water table height. Changes in storage for a fully saturated soil are due mainly to the compression of the soil matrix (Narasimhan, 1979). Concepts and techniques useful for modeling salt marsh peat are the concepts and techniques applied to deep confined aquifers. This leads to some interesting results with regards to the processes controlling infiltration.

2.1 Stress Relationships

When the compression of the soil matrix becomes an important factor in the storativity of a soil, as is the case with salt marsh peat, then the flow of water is coupled with the distribution of stress in the soil. Therefore, it is appropriate to preface the presentation of principles of fluid flow in a saturated porous medium by a discussion of the role of the fluid in stress relationships within the soil.

Soil is composed of three phases, a solid phase consisting of an open structure of particles with fluid and gaseous phases present in the pore spaces. In peat, the solid phase consists of fine sand, silt, and clay sized particles. Organic matter is present both as part of the solids and suspended and dissolved in water, the liquid phase. Consistent with observations that peat is saturated or nearly so, the gas phase, air, is assumed to be absent or present only in negligible amounts.

Stresses in a saturated soil are shared between the fluid phase and the solid phase. Consider the normal stresses on a horizontal plane due to a vertical load acting on the column of soil shown in figure 2.1. The total stress σ_T is divided as follows:

$$\sigma_T = m\sigma_G + (1-m)p \qquad [2.1]$$

in which σ_G is the average stress on the particle to particle interface, p is the pressure in the fluid, and m is the average proportion of a cross section taken up by particle to particle contact. Compressive stresses have been defined as positive. For very small particles, such as clays, interparticle forces may be transferred entirely due to surface chemistry effects, and the area of actual particle-to-particle contact is zero (Lambe and Whitman, 1969). The concept that part of the total stress is being carried by the interaction of solid particles is still valid in this case. The interparticle stress is referred to as the effective stress σ' and the total stress equation is written as:

$$\sigma_T = \sigma' + p \qquad [2.2]$$

where it has been recognized that m is small so that $(1-m) \sim 1$. Notice that equation 2.2 is valid only when referring to the average stress on an area large enough to contain many interparticle connections.

Both water and the assemblage of solid particles respond to an increase in stress by decreasing their volumes. This response can be expressed by a compresibility factor (Bear, 1972), the ratio of the increment of strain to the increment of stress:

$$\beta = \frac{-1}{U_b}\frac{dU_b}{d\sigma} \qquad [2.3]$$

Figure 2.1 Stress Distribution in Soil

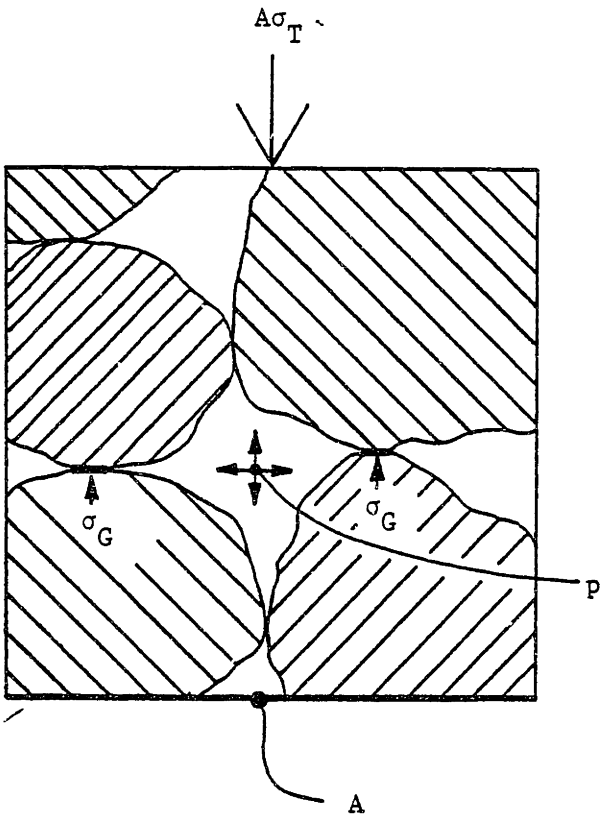

where U_b is the bulk volume of a given mass of the material and includes the volume of the enclosed pore space when referring to the soil compressibility. It is a good first approximation to assume that the straining of the soil matrix is due entirely to a decrease in the enclosed pore volume. Therefore, for a fully saturated soil the strain in the fluid phase is related to the strain in the solid matrix by the ratio of fluid volume to total volume, n.

Suppose that a load is applied to the soil uniformly on a horizontal plane causing a strain ε and that no fluid is lost in the process. The increment in total normal stress σ_T^* is, by equation 2.2,

$$\sigma_T^* = \frac{-1}{\beta_s}\varepsilon + \frac{-1}{n\beta_w}\varepsilon \qquad [2.4]$$

where β_s and β_w are the compressibilities of the soil matrix and water respectively. The first term on the right hand side of equation 2.4 is the increment in effective stress, and the second term is the increment in the pore pressure. The porosity of peat n is high, say 0.9, and the compressibility of water ($\beta_w \sim 5.10^{-11}$ cm^2/dyne) is about five orders of magnitude less than the compressibility of the solid matrix. Therefore, for an increment in total stress σ_T^* on a saturated soil in which water is not lost, virtually all of the added stress is carried by an increase in pore pressure, and for reasonable increments in stress the straining of the soil will be negligible.

The condition that no water be lost from the soil while the total normal stress is increased is approximated in fine grained soils in which water flow is inhibited. Water flows freely in coarse sands and

gravels, so here the increment in the normal stress will be transferred to the intergranular stress immediately. If after an increase in stress in a saturated fine grain soil the fluid is allowed to drain (due to an induced pressure drop across a boundary for example) then the soil matrix will collapse and the stress increment will be transferred to the effective stress component. This process is known as consolidation. Consolidation can also be caused by the withdrawal of pore water from the soil in the absence of an increase in total stress and is partially reversible by forcing water back into the soil.

The convention adopted in the field of soil mechanics for representing the consolidation of a soil is to define the void ratio e as a function of effective stress. The void ratio is defined as the ratio of the volume of pore space to the volume of solids in a soil. The relationship between e and σ' is determined experimentally and either a linear relation or a logarithmic relation is used to fit the data.

2.2 Basics of Fluid Flow

The basic relation for fluid flow through a porous medium is Darcy's Law which states that the discharge per unit area of porous material is proportional to the gradient in the piezometric head of the fluid parallel to the direction of flow.

$$q = -K \, d\phi/dx \qquad [2.5]$$

Darcy's Law was first established empirically in 1856. Bear (1972) summarizes attempts since then to derive Darcy's Law from first

principles. As with the stress relations, Darcy's Law is valid for fluid flows averaged over some finite volume of material.

The piezometric head of water at a point is defined by

$$\phi\,(x,y,z) = z + \frac{1}{\gamma_w}\,p(x,y,z) \qquad [2.6]$$

where $p(x,y,z)$ is the pore pressure at the point and γ_w is the unit weight of water. The piezometric head is sometimes also called the hydraulic potential, and here it will be referred to simply as the potential or piezometric potential.

The constant of proportionality K in equation 2.5 is known as the hydraulic conductivity and it depends on both fluid and soil matrix properties in the following way:

$$K = \frac{kg\rho}{\mu} \qquad [2.7]$$

Here g is the acceleration due to gravity, ρ and μ are the density and viscosity of the fluid. The factor k has units L^2 and is a measure of the pore size distribution and shape. The hydraulic conductivity depends on the degree of saturation of the material and the amount of strain in the soil matrix through its dependence on k. Desaturation occurs in the largest pores first, thus affecting the distribution of pore sizes involved in the fluid flow, and compression of the soil occurs mainly by reducing pore volume. Hydraulic conductivity also varies spatially (heterogeneous) and with flow orientation (anisotropic).

Darcy's Law, the principle of conservation of fluid mass, and the stress relationships discussed in section 2.1 are sufficient to derive the governing equation for the flow of a water in a saturated porous medium, peat. This is done in the appendix with the following result for flow in one dimension:

$$\frac{\partial \phi}{\partial t} = \alpha \frac{\partial^2 \phi}{\partial x^2} \qquad [2.8]$$

$$\alpha = \frac{K}{(1-n)\gamma_w a_v}$$

in which n is the porosity of the porous material and a_v, the coefficient of compressibility, is the slope of a linear relation for the void ratio e in terms of the effective stress σ'.

The following assumptions have been made in the derivation of equation 2.8:

1) incompressible fluid,
2) fully saturated porous medium,
3) constant volume of the solid phase,
4) constant total stress at a point,
5) negligible change in the elevation of a point due to the compression of the soil matrix,
6) void ratio linearly related to effective stress with constant of proportionality a_v,
7) constant, homogeneous hydraulic conductivity.

The assumption of constant, homogeneous hydraulic conductivity is necessary in order to produce a relation amenable to analytic

solutions. The variation of the hydraulic conductivity of salt marsh peat with varying effective stress or position is not known, so the assumption is somewhat justified on the grounds of ignorance. The effect of this assumption on the analysis of the flow regime will be dealt with in detail later.

The solution of flow problems with equation 2.8 requires the specification of two boundary conditions and an initial condition expressed in terms of the potential ϕ. Assumption number 4 above essentially provides the solution to the coupled stress problem. Common boundary conditions are specified flux across a boundary $\partial\phi/\partial x|_b$ and fixed potential at a boundary $\phi|_b$. Solutions can be obtained for semi-infinite problems by replacing the boundary condition at infinity by the constraint that the solution for ϕ be bounded where defined. The description of the interface between the pore water and the atmosphere requires a mixed boundary condition. Zero pressure is exerted on the water at the boundary, amounting to a fixed potential boundary. When the pore pressure inside the soil is greater than atmospheric then water will flow out and a condition known as a seepage face is created. When pore pressures are less than atmospheric, surface tension at the interface maintains a pressure discontinuity, and the boundary becomes a zero flux boundary.

The role of surface tension at the pore water-atmosphere boundary can be understood by using a capillary tube as an analog for the pores of a soil, see figure 2.2. The pressure drop Δp across the air-water interface in a capillary tube is given by:

Figure 2.2 Capillary Tube Analog

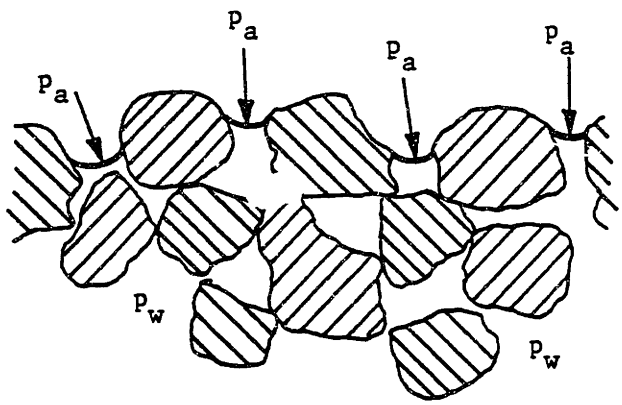

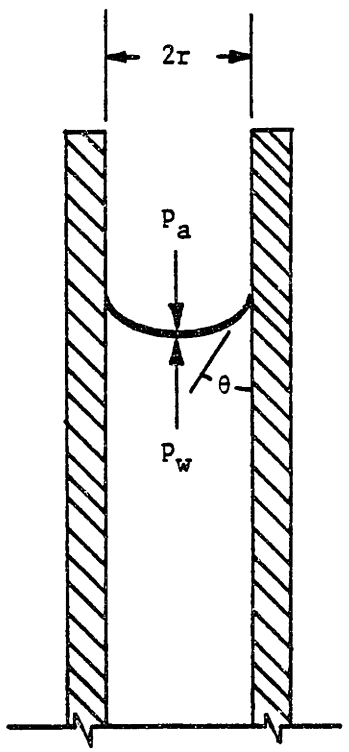

$$\Delta p = p_a - p_w$$

$$\Delta p = \frac{2\sigma_s}{r} \cos\theta \qquad [2.9]$$

in which σ_s is the tension in the water surface. The wetting angle θ depends on the adhesion between water and the material forming the side of the capillary tube. The pressure drop is the result of the surface tension σ_s acting through a curved surface. The curvature of the surface is controlled by the pore geometry, represented by the radius of the capillary tube in the analog. The pore geometry of a soil controls initiation of desaturation by controlling the maximum pressure drop that can be maintained across the pore water atmosphere interface. The maximum sustainable pressure drop is known as the air entry value of the soil, and since pressure is usually defined relative to atmospheric, the air entry value of a soil is usually defined as the pore pressure at which desaturation begins.

2.3 Mechanism for Infiltration

The mechanics of a saturated porous medium during the process of infiltration can be represented by the mechanical system consisting of a piston and cylinder, a spring, and a valve shown in figure 2.3. The cylinder filled with water represents the saturated soil. Stresses on the soil are carried partially as effective stress acting within the soil matrix (the spring) and partially as pore pressure in the water. The pressure in the cylinder is described completely by the pressure acting on the underside of the piston p_w and the assumption that the pressure distribution within the cylinder is hydrostatic. The valve represents the boundary condition at the pore water-atmosphere interface. Since the water table in the marsh is located below the surface, the pore pressure at the peat surface

Figure 2.3 Mechanism for Infiltration

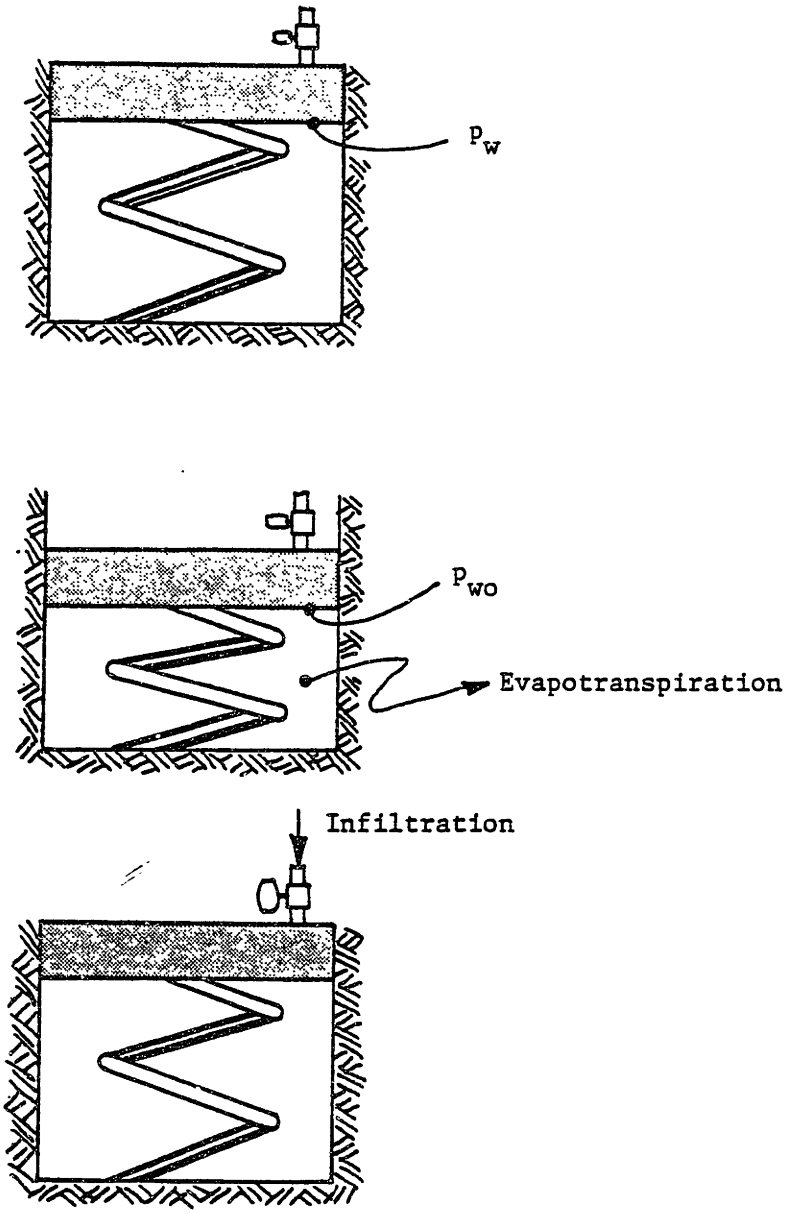

p_w will be less than atmospheric. The closed valve then plays the role of the surface film, and it is assumed that the air entry value is never reached. The rate of flow through the opened valve is assumed to be proportional to the pressure drop across it in analogy to Darcy's Law. If water is removed by evapotranspiration or drainage when the soil surface is dry (valve closed), the spring is compressed as the volume of the cylinder decreases due to the loss of water. Compression of the soil matrix causes more of the total stress on the soil to be transferred to the effective stress component and the pore water pressure decreases to p_{wo}.

Infiltration occurs in the salt marsh when rising tides flood the peat surface. Consider for the purposes of illustration that water floods the surface of the marsh instantly to a depth h and that the surface remains flooded indefinitely. The additional stress on the soil due to flooding is $\gamma_w h$, and this stress increase is transferred instantly to the water phase by the mechanism described in section 2.1. Since water is present on both sides of the soil boundary there is no longer any surface tension effect and water flows into the soil in response to a pressure drop across the valve given by:

$$\gamma_w h - (p_{wo} + \gamma_w h) = -p_{wo} \qquad [2.10]$$

The soil matrix expands due to the changes in pore water volume and pore pressures increase. Water will continue to infiltrate into the soil until the water pressures at the interface equalize, $p_w = \gamma_w h$. If the marsh surface is then drained instantaneously, the change in stress at the surface is again transferred immediately to the pore

water, and the pore pressure at the surface drops to zero.

Notice that in this idealized flooding event the infiltration is controlled by the pressure difference present at the soil surface before the flooding takes place. The pressure due to the depth of ponding on the surface simply adds to the pore pressure uniformly and, therefore, does not contribute to the flow of water through the valve. In fact, the pore pressure response to flooding can be divided into two components, a dynamic component that rises due to the increased pore water volume and a static component due entirely to the depth of water ponded on the surface. The response of the dynamic component contains all of the information about the flow of water into the soil.

An actual infiltration event differs from the idealized case in several ways, but the mechanism is the same. The surface of the marsh floods gradually with the ponding depth varying in time. It can be imagined, however, that the changes in ponded depth occur incrementally, and the arguments employed above can be used to show that the "static" component of the pore pressure simply varies with the depth of flooding. The pressure distribution in the salt marsh peat will not generally be hydrostatic. Deviations from a hydrostatic distribution will occur if there is evapotranspiration occurring at the time of flooding. Typical flux rates in the peat for evapotranspiration are on the order of 1.5×10^{-5} cm/s during the day (Hemond and Fifield, 1982). Fluxes in the peat due to infiltration are on the order of 1.5×10^{-4} cm/s. The deviation of the pressure distribution from

hydrostatic is proportional to the flux, so relatively speaking the deviation of the pressure distribution in the infiltration problem due to evapotranspiration is small. The period of flooding in the marsh is not long enough to drive the infiltration process to equilibrium. Therefore infiltration in the field is a function of the pressure drop at the surface before flooding and the length of time that the surface is flooded.

Using the definition of the potential, equation 2.6, and the definition of the dynamic and static components of pore pressure discussed above, dynamic and static components of the potential can be defined. The flow of fluid in peat during infiltration depends only on the response of the dynamic component of the potential. From the description of the mechanics of infiltration it is evident that the boundary condition on the dynamic potential is a step increase of p_{wo}/γ_w applied at the time of first flooding when the surface tension effect at the boundary is broken. The solution of equation 2.8 for a step increase in potential ϕ_o on the surface of a deposit of peat of depth L with an impermeable lower boundary is, from the appendix,

$$\phi(x,t) = \phi_o\left[\mathrm{ERFC}\left(\frac{2L - x}{\sqrt{4\alpha t}}\right) + \mathrm{ERFC}\left(\frac{x}{\sqrt{4\alpha t}}\right)\right] \qquad [2.11]$$

This relation will be used in the interpretation of field observations in chapter 3.

3.0 Laboratory and Field Observations

The principles of fluid flow in a saturated porous medium have been discussed in Chapter 2. When certain conditions are met, the flow of water in salt marsh peat is described by the following partial differential equation:

$$\frac{\partial \phi}{\partial t} = \alpha \frac{\partial^2 \phi}{\partial x^2}$$

$$\alpha = \frac{K}{(1-n)\gamma_w a_v}$$

Here ϕ is the hydraulic potential, and γ_w is the unit weight of water. Parameters describing the peat are the hydraulic conductivity K, the porosity n, and the coefficient of compressibility a_v.

Samples of peat from the Great Sippewissett Marsh have been obtained in the form of cores taken throughout the marsh. Laboratory techniques have been developed to measure the peat parameters K, n, and a_v from the core samples. Field observations of hydraulic potential, infiltration, and water exchange between the peat and the creeks across the creek bank have been made. Both the laboratory and field observations are summarized in this chapter. The field observations of hydraulic potential and infiltration, and the laboratory derived peat parameters are used to verify the theoretical mechanism for infiltration presented in section 2.3.

3.1 Hydraulic Conductivity of Peat

The peat sampling program in the Great Sippewissett Marsh and the determination of hydraulic conductivity are described by Fifield (1981). Cores spanning the full depth of the peat were taken at 19 sampling stations. The peat ranged in depth from 40 centimeters to 240 centimeters. Vertical hydraulic conductivity was determined in the laboratory using the falling head method described by Lambe (1951). In situ determination of horizontal conductivity was performed at six of the sampling stations using a constant head pumping procedure described in the Earth Manual, U.S. Department of the Interior, Bureau of Reclamation.

Three full depth peat cores were collected in connection with a piezometer transect installed in the Sippewissett Marsh during August 1981. Hydraulic conductivities at eight locations in the vertical section of peat instrumented with piezometers were determined from these cores using the method described by Fifield (1981). The hydraulic conductivity of the underlying clay was also determined.

A 50 centimeter horizontal core was collected 50 centimeters from the surface at the creek at the 1981 piezometer transect, and its hydraulic conductivity was determined in the laboratory. This was done in an attempt to observe any anisotropy (variation with orientation) in the hydraulic conductivity of peat. Anisotropy in hydraulic conductivity is a common phenomenon in deposited materials. It is due largely to the fact the flow across layers is inhibited relative to flow parallel to layers when a less permeable material is

interbedded with a permeable one, clay in sand for example. Variation in the hydraulic conductivity of the horizontal cores from the conductivity of the vertical cores at the 1981 transect is not significant compared to the variation observed between the vertical cores. Fifield (1981) estimates a horizontal conductivity to vertical conductivity ratio of 1.3 to 2.6 on the basis of comparison between her laboratory results (vertical) and field test results (horizontal). This is small compared to an observed range in vertical hydraulic conductivities of 2.6×10^{-6} cm/s to 6.3×10^{-2} cm/s.

3.2 Compressibility of Peat

The relation between void ratio and effective stress in salt marsh peat was explored using the consolidation test procedure outlined by Lambe (1951). Peat samples were taken from the cores collected for hydraulic conductivity determination. Samples were taken at the nominal depths of 1, 2, 3, 5, and 7 feet, length of the core allowing, at all sampling stations. A total of 53 samples of Sippewissett Marsh peat were tested.

Testing a peat sample consists of the following steps. A 3.75 cm long sample is cut from the core; the coreliner is retained with the sample to constrain horizontal deformation. The sample is saturated and held at full saturation throughout the procedure by immersing it in a water bath. Porous plates are placed in contact with each horizontal peat face to assure that the sample is well drained. The sample is then loaded to desired stress levels and the corresponding change in volume after drainage is observed directly

with strain gages. The peat sample response at five stress levels was observed.

At the end of the series of loadings, the peat sample is dried to constant weight at 85°C to determine the void volume from the volume of water lost. The specific gravity of the remaining material is determined so that values for porosity n and initial void ratio e can be determined using volumes and weights recorded before beginning the test. The void ratio at each load level is determined from the initial void ratio and the observed volume changes.

The response of soils to a consolidating stress depends on the stress history of the material. At stresses less than the maximum past stress the response is more or less elastic, although some hysteresis may be observed. At stresses exceeding the maximum past stress the change in void ratio with increasing stress is greater than the change at stresses below the maximum past stress. This is due to inelastic deformation of the material under the greater stress. As stresses decrease from the new maximum stress a new range of elastic response will be observed. Salt marsh peat is stressed repeatedly over the same stress range, so the relation of void ratio to effective stress in the elastic range is desired. The corresponding stresses are small, on the order of tenths of an atmosphere.

The empirical relation between void ratio and effective stress determined by the consolidation test is commonly described by fitting either a linear or logarithmic function to the data. The logarithmic

function is the more widely used in the field of soil mechanics, and it has the form:

$$e = C_c \log \sigma' + C \qquad [3.1]$$

The coefficient C_c is known as the compression index. In order to use a linear equation of flow, equation 2.8, it is necessary to fit a linear relation to the data:

$$e = a_v \sigma' + C \qquad [3.2]$$

where a_v is the coefficient of compressibility. The coefficients of compressibility obtained from the Sippewisset Marsh peat ranged from 3×10^{-5} to 5×10^{-7} cm s^2/gm. Porosities of the peat ranged from .93 to .30.

3.3 Distribution of the Peat Parameters

The influence of peat on the flow of water through it is reflected by two parameters in the equation of flow, the hydraulic conductivity K and the storativity due to compressibility, $(1-n)\gamma_w a_v$. Spatial variations in these parameters will be reflected in the flow patterns that occur, so the distribution and variability of the peat parameters must be addressed. Fifield (1981) observed a three zone structure in the hydraulic conductivity with depth. A surface zone, corresponding to the rooting zone, exhibits a relatively low hydraulic conductivity as does a zone of peat directly above the underlying deposits of sand and clay. The middle zone of peat is more permeable than the bounding zones by at least an order of magnitude. Fifield (1981) also observes a correlation between hydraulic conductivity and relative density of the peat. Relative density is the ratio of saturated density to the density of water, so it is a measure of the

porosity of the peat and the amount of inorganic solids. The three zone structure also was observed in the cores taken at the 1981 piezometer transect. There was a clear demarcation between the root zone and the underlying peat. The root zone peat appeared light brown in color and very firm. The peat immediately below the root zone was dark in color and much less firm when cored.

The reduced hydraulic conductivity at depth is probably due to higher mineral content of the peat there. This peat would have been the first to form as the result of the colonization of a mud or sand flat by salt marsh vegetation. Redfield (1972) has observed that newly colonized areas build peat quickly by incorporating a relatively large amount of trapped sediments.

The laboratory procedures described in sections 3.1 and 3.2 have been used to obtain the hydraulic conductivity and compressibility of 52 peat samples. The percent organic content by dry weight was also determined by combustion. The distributions of hydraulic conductivity and the compressive storativity are shown as frequency polygons of $-\log K$ and $-\log (1-n)\gamma_w a_v$ in figures 3.1 and 3.2. The distributions are symmetric and the proportions of observations that fall within the range described by the mean plus and minus the standard deviation of the logarithms are .69 and .74 for the hydraulic conductivity and the storativity respectively. The proportion in this range for the normal distribution is .68, so both hydraulic conductivity and compressive storativity appear to be approximately log-normally distributed. The log-normal distribution of hydraulic conductivity has

Figure 3.1 -Log K Frequency Polygon

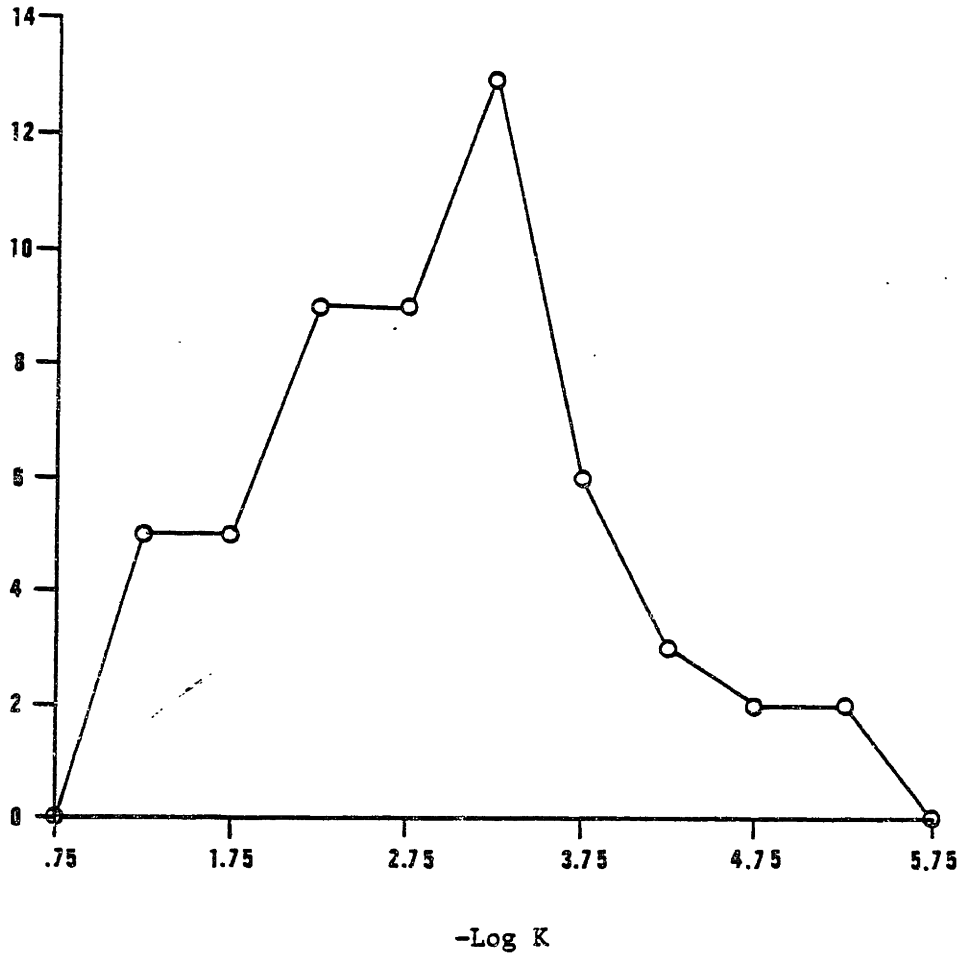

Figure 3.2 -Log $((1-n)\gamma_w a_v)$ Frequency Polygon

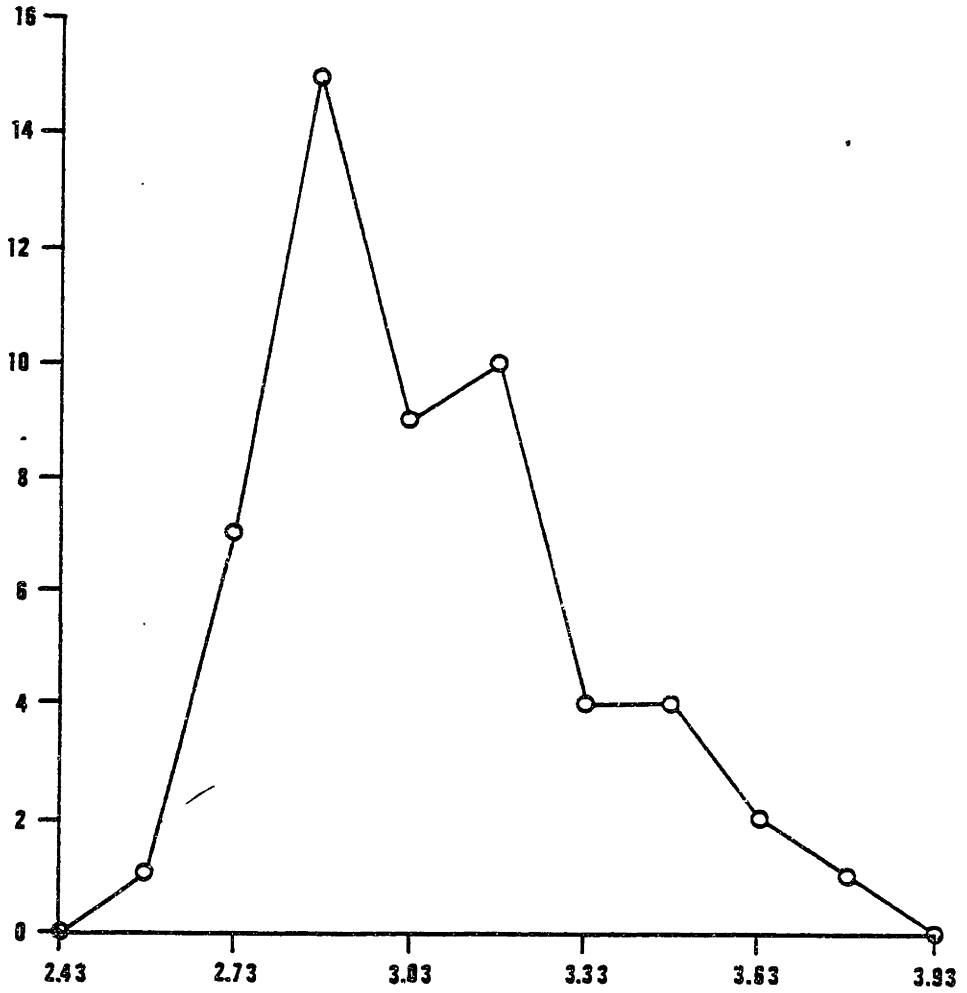

been observed in many different materials (Freeze and Cherry, 1979).

The means and standard deviations for various subsets of the data are presented in table 3.1. The zoned structure of the peat is evident in the organic content data. The low organic content in the lower 30 cm of peat indicates that the mineral content (silts, sands, and clays) is fairly high there as suspected on the basis of marsh building processes (Redfield, 1972). An order of magnitude change in hydraulic conductivity between the root zone and the underlying peat is also indicated. The distinction between the conductivity of the peat in the root zone and the peat immediately beneath it may be even greater than suggested by these figures since the non-root zone peat lumps the permeable middle layer together with the less permeable lower layer. The compressive storativity does not seem to vary with depth.

The storativity always appears in the mathematical description of the flow problem in the denominator of the ratio:

$$\alpha = \frac{K}{(1-n)\gamma_w a_v} \qquad [3.3]$$

Therefore, it will be convenient to define α as the second of two peat parameters, with K. The distribution of log α is shown in figure 3.3. It also approximates a log-normal distribution and has a mean logarithm of 0.13 and a standard deviation of 0.979. The standard deviation of log K is much greater than the standard deviation of log $(1-n)\gamma_w a_v$. This results in log α being highly correlated with log K as shown in figure 3.4. At least squares fit leads to the following relation:

$$\log \alpha = 2.82 + .929 \log K \qquad [3.4]$$

Table 3.1 Summary of Peat Parameters

	-Log K		-Log $(1-n)\gamma_w a_v$		% Organic	
	mean	σ	mean	σ	mean	σ
Root Zone (upper 30 cm)	3.51	.826	3.11	.191	38.5	11.3
Non-Root Zone	2.74	.996	3.02	.297	-	-
Lower 30 cm	-	-	-	-	9.4	11.8
Overall	2.93	1.01	3.03	.268	25.6	20.0

Figure 3.3 Logα Frequency Polygon

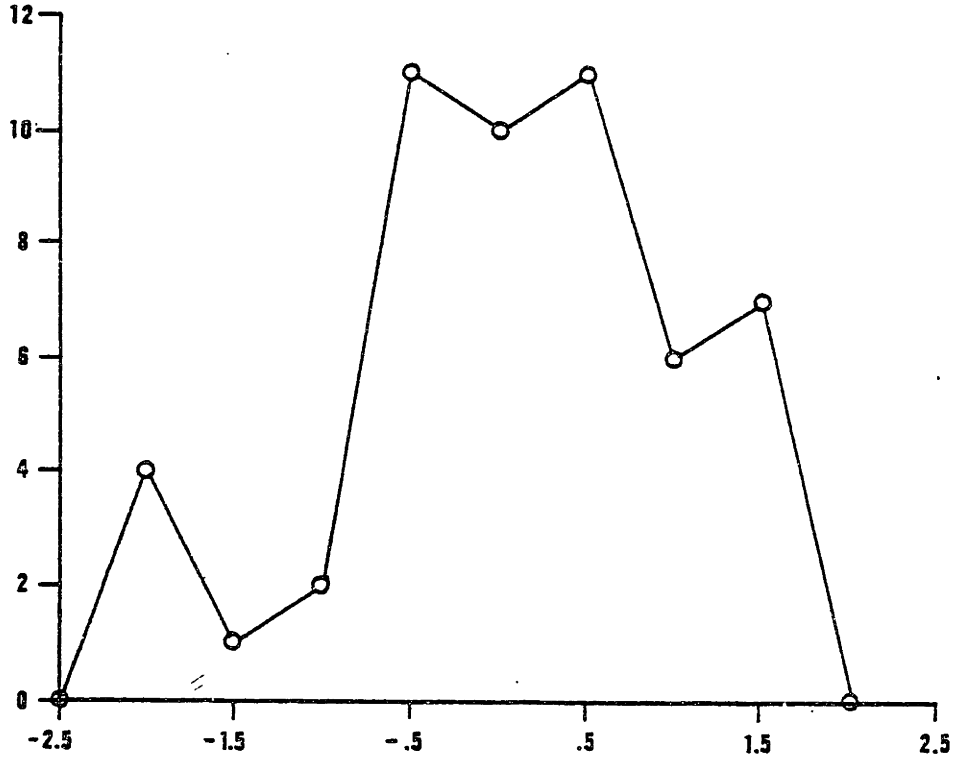

Figure 3.4 Correlation of Log α with -Log K

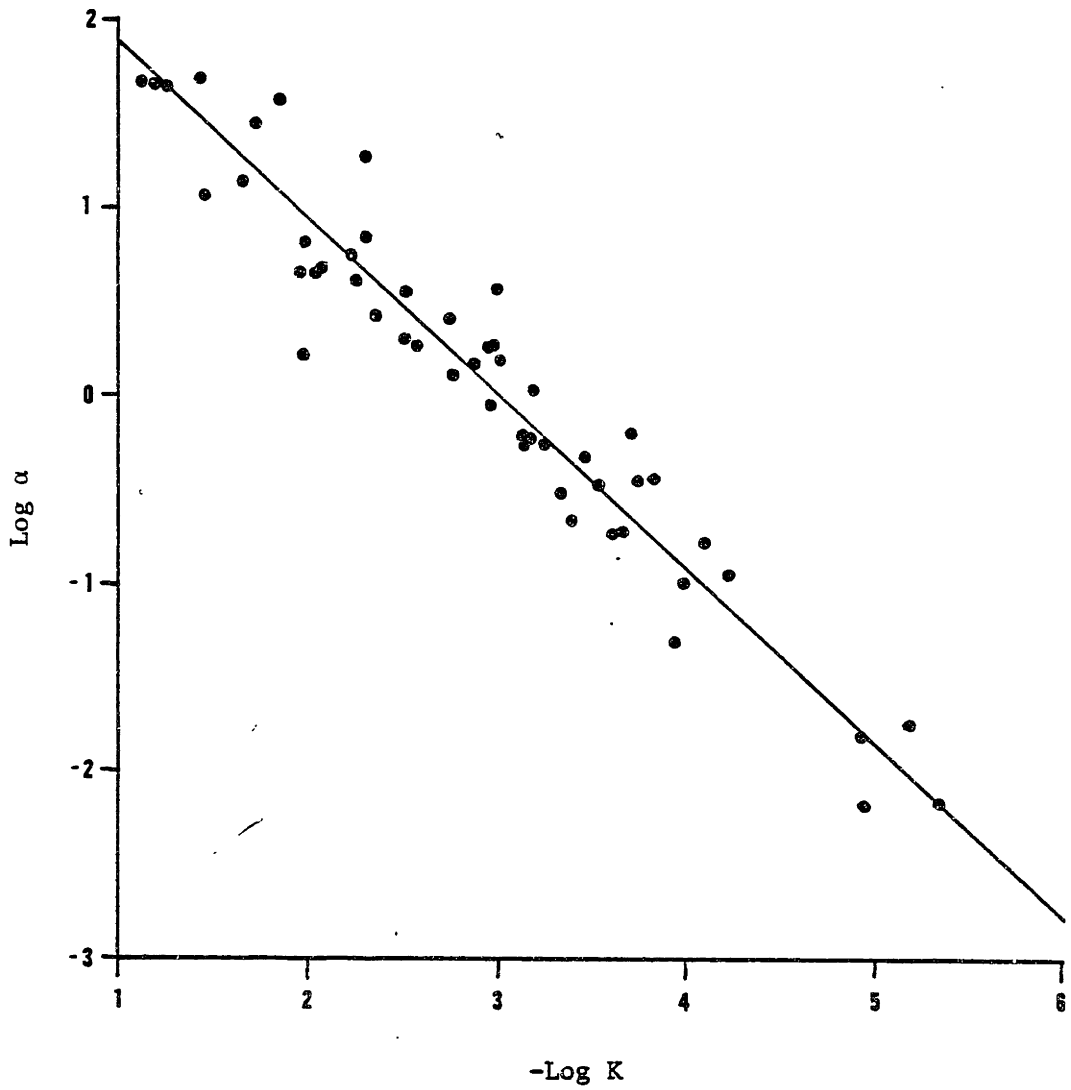

The correlation coefficient for this relation is .970.

The peat parameters in the flow equation, K and α , are seen to be spatially distributed in a three zone vertical structure. This distribution can be represented in the formulation of flow problems. However, there is also a good deal of random variability that can not be explicitly represented. The random variability of the peat parameters introduce uncertainty into the results of the analysis of the flow of water in peat. The variability of the parameters can be represented by using a range of values in the flow analysis. The result of an analysis approached in this way is a specified range of predictions representing the uncertainty of the results.

The variation in the two peat parameters is dominated by the variability of the hydraulic conductivity. The range of parameters to be used in the flow analysis will be defined by the mean plus and minus the standard deviation of the logarithm of the hydraulic conductivity. The hybrid peat parameter α is highly correlated with hydraulic conductivity, so equation 3.4 can be used to define variations in α in terms of the corresponding variations in hydraulic conductivity.

3.4 Field Measurements of Water Fluxes

Direct measurements of surface infiltration into the peat due to tidal flooding and the exchange of water between the creeks and the peat across the creek banks have been made. The surface infiltration measurements were made with a device described by Hemond and Burke (1981). The device isolates an area of the marsh surface, which is

subject to flooding, with an enclosure. A water level sensor is connected to a recording pump so that as the surrounding marsh surface floods water is pumped into the enclosure at a rate sufficient to keep the water level above the enclosed peat surface nearly equal to the water level above the surrounding peat. The pump is reversible, so when the surrounding marsh drains the pump drains the enclosure. The amount of water pumped and the direction of pumping is known, as is the enclosed surface area. So, the net infiltration during a flooding event can be calculated. Infiltration measured by this technique ranged from 2 cm to 0 cm per event. Most measurements were less than .5 cm per event, below the estimated sensitivity of the technique.

The exchange of water across the creek bank and creek bottom was measured with a device described by Lee (1977). A section of creek bank is isolated by driving a shallow open ended cylinder into the peat. The end of the cylinder above the peat in the creek is closed except for a valved or stoppered opening. A plastic bag is connected to this opening with a hose. The bag and the cyliner are completely full of water and the bag is immersed in the creek. The bag and the barrel define a volume of water that can be changed only by flow into or out of the peat. The exchange of water across the peat face is still controlled by the water pressures in the creek which are allowed to act through the plastic bag. The volume of water trapped within the cylinder is constant, so integrated flux measurements can be obtained by measuring changes in the volume of water in the bag during measured periods of time.

Measurements of fluxes across the creek banks were made at several locations in the Sippewissett Marsh. It will be shown later that fluxes across a surface of a porous medium due to a periodic potential forcing are 1/8 of a period out of phase with the potential (creek level). Unfortunately, this was not known at the time that the flux measurements were made with the result that some measurements span the period during which the direction of flux changed. The flux measurements are further complicated by steady state fluxes in response to surface flooding and evapotranspiration. The measurements do, however, establish that the exchanged volume due to tidal forcing in the creeks is on the order of several centimeters.

3.5 1981 Piezometer Transect

A piezometer transect was established in the Great Sippewissett Marsh during August, 1981. Four piezometer stations were installed along a line perpendicular to a creek as shown in figure 3.5. Four piezometers were installed at each of the first three stations located 1, 4.5, and 8.5 meters back from the creek. The fourth station, 12 meters from the creek, had only one piezometer. The nearest upland region was 30 meters from the creek. The piezometers were screened at nominal depths of 1, 2, 4, and 5 feet. This arrangement of the piezometers was designed to reveal the flow pattern in the peat near the creek bank.

The piezometers were constructed of nominal 1/8 inch brass pipe and 3/4 inch stainless steel Johnson screens. The length of the screens was 15 cm. An acoustic device was used to automatically

Figure 3.5 1981 Piezometer Transect

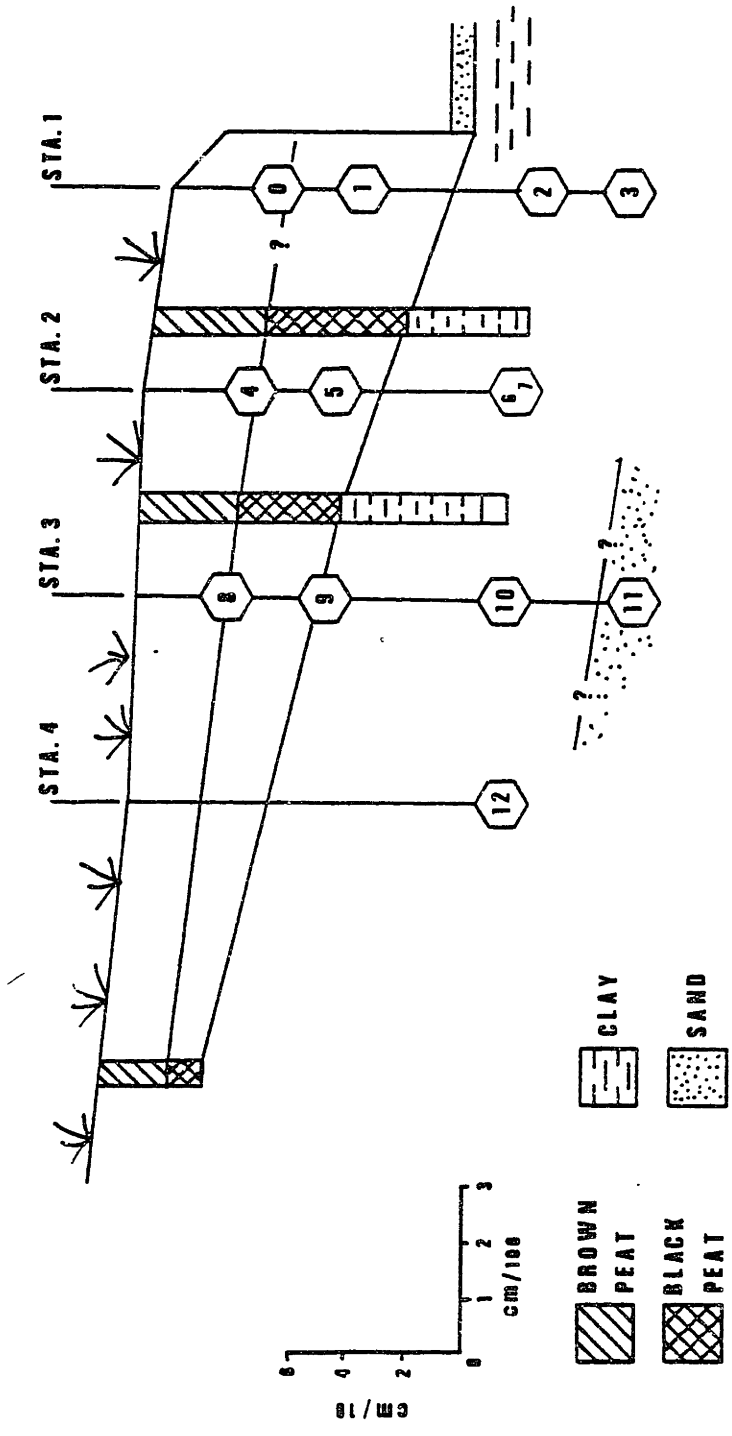

measure and record the water levels in the piezometers. The recording device and the installation procedure for the piezometers are described by Hemond (1982). Using this approach, a water level reading was taken at each of the 16 wells used (13 in the peat, 1 in the creek, and 2 control wells) every 160 seconds. The readings were recorded on digital cassettes in the field. An Altair 8800b microcomputer was used to read and interpret the data on the cassettes in the laboratory.

Piezometer observations were made at the 1981 piezometer transect on three consecutive days in August. High tides flooded this area of the marsh on all three days. The observations spanned a complete tidal period on two of the days, and these data have been averaged over the tidal cycle at each well. The averaged piezometer readings have been used to plot equipotentials in figures 3.6 and 3.7. Notice that the vertical to horizontal scale expansion has the effect of distorting the equipotentials so that they seem more vertically oriented. A shift in the equipotentials from one day to the next corresponding to a 40 cm decrease in the averaged potentials was observed. This suggests that water movement near the creek banks has a component with a period longer than the 12.5 hour tidal period.

Peat cores taken along the transect after the piezometer observations were made and observations at the time of piezometer installation suggest the peat structure shown in figure 3.5. Laboratory measurements of hydraulic conductivity of the peat cores revealed the three zoned distribution of hydraulic conductivity observed by Fifield (1981) that was discussed earlier in section 3.1. The hydraulic

Figure 3.6 Averaged Piezometric Potentials; August 5

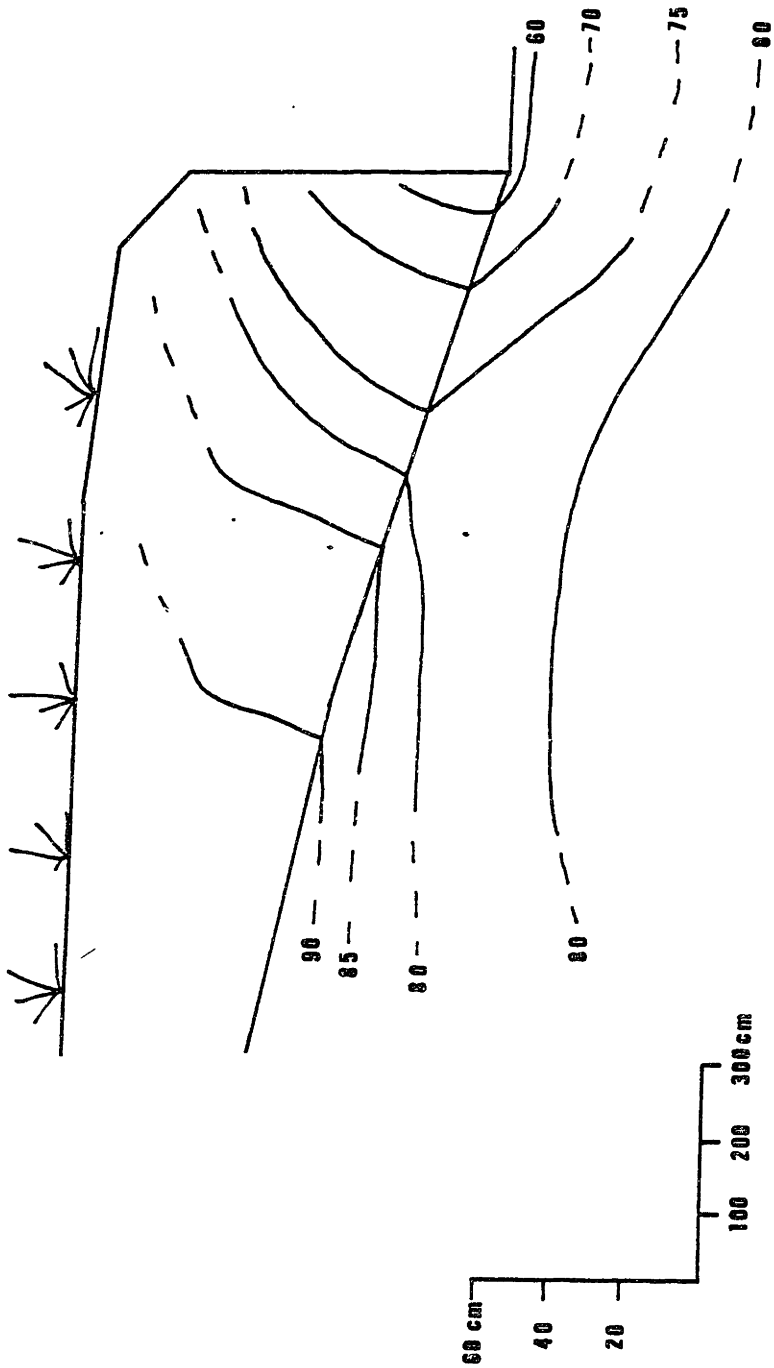

Figure 3.7 Averaged Piezometric Potentials; August 6

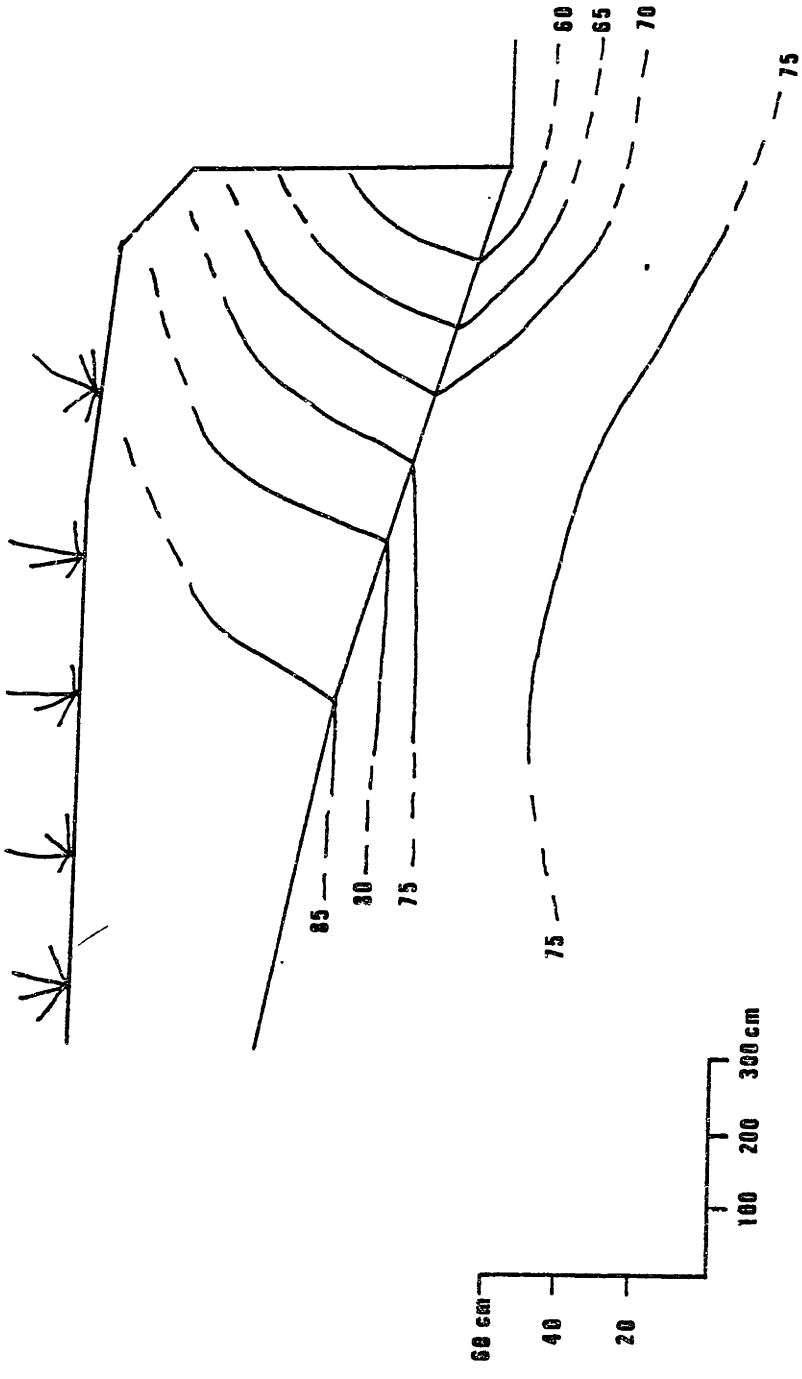

conductivity in the root zone, the light brown peat, is 6 x 10^{-4} cm/s. The hydraulic conductivity in the dark peat ranges from 2 x 10^{-3} cm/s directly beneath the root zone to 1 x 10^{-4} cm/s above the clay. The clay has a hydraulic conductivity of 7 x 10^{-6} cm/s. The piezometer measurements suggest that the clay is connected, perhaps by interbedding, with the sand layer observed below the peat in other areas of the marsh. The effect of the zoned hydraulic conductivity distribution on the flow patterns in the peat can be seen in the equipotential plots in figures 3.6 and 3.7. The direction of water flow is perpendicular to the equipotentials. The distortion of the scales distorts the flow pattern by accentuating the horizontal component. The figures show that horizontal flow is present mainly in the more permeable peat at depth.

3.6 Infiltration Rates Inferred from Piezometer Readings

The piezometer readings of the near surface piezometers in the 1981 transect show the response of the piezometric potential to infiltration during flooding by high tides. The theory of infiltration into a saturated soil, presented in section 2.3, divides the potential response into a static and dynamic component. The static component of the potential response is due to the increase in vertical stress in the peat caused by water ponding on the surface. The dynamic component is caused by redistribution of stress from effective stress to pore pressure as the soil expands to accomodate the volume of infiltrated water. Both components of the piezometric potential response can be seen in the response of piezometer 4 to flooding at high tide on August 5 (see figure 3.8). The static response dominates,

Figure 3.8 Piezometer Response to Inundation

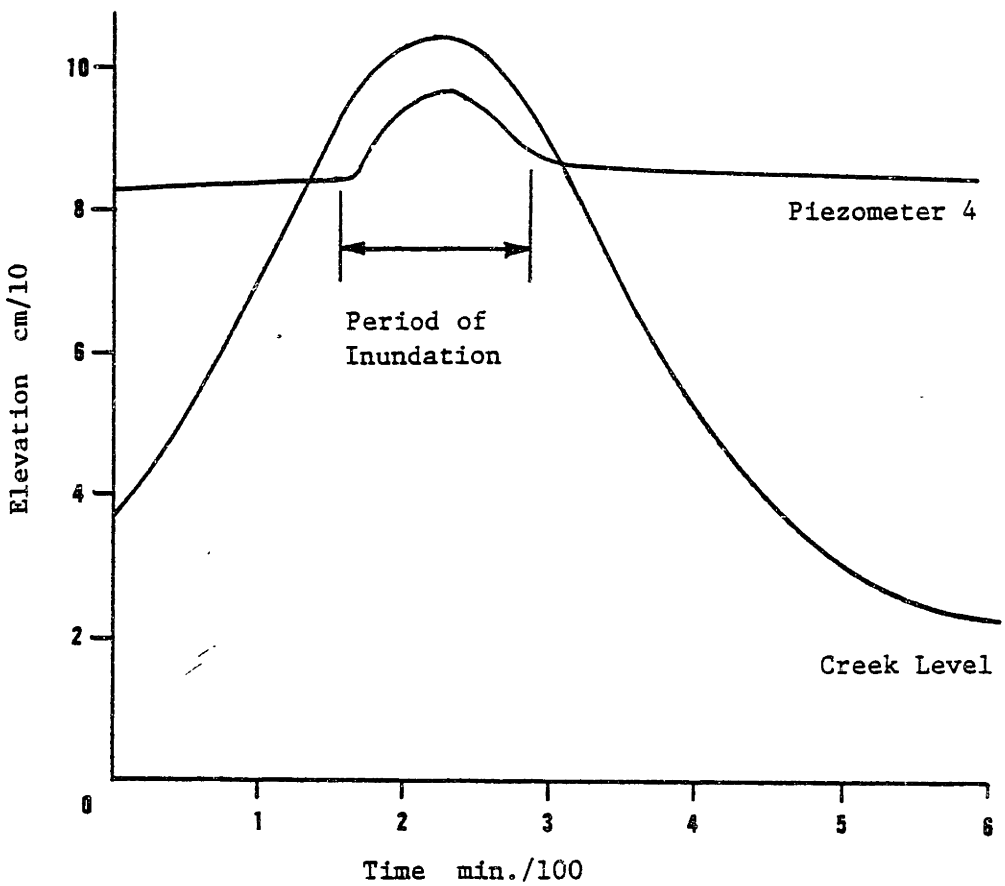

causing the piezometer readings to peak with the level of the tide. The dynamic response is responsible for a 4 cm increase in the piezometer reading during the period of flooding.

The dynamic potential response to infiltration is modeled by the response to a step increase in potential at the peat surface. For a finite depth of peat underlain by an impermeable layer, the increase in the dynamic potential is given by:

$$\phi^{*}(x,t) = \phi_o \left[\mathrm{ERFC}\left(\frac{x}{\sqrt{4\alpha t}} \right) + \mathrm{ERFC}\left(\frac{2L - x}{\sqrt{4\alpha t}} \right) \right] \qquad [3.5]$$

where $\alpha = \frac{K}{(1-n)\gamma_w a_v}$. The magnitude of the step increase ϕ_o is the pressure drop across the pore water-atmosphere interface divided by the unit weight of water γ_w. By assuming a hydrostatic pressure distribution in the peat, ϕ_o can be estimated as the difference between the elevation of the marsh surface at the piezometer station and the elevation of the water in the piezometer before flooding of the surface. In general, the presure distribution in the peat will not be hydrostatic due to evapotranspiration fluxes, but deviations caused by evapotranspiration are expected to be small.

The depth of ponding during flooding can be estimated to perhaps ±.5 cm by extrapolating the water surface elevation from readings taken in the creek. Therefore, the dynamic piezometric potential response can be estimated from recorded piezometer readings. This has been done for the near surface piezometers for flooding events observed on August 5 and August 6, and the observed dynamic potential responses are plotted in figures 3.9 - 3.13. The time scale begins

Figure 3.9 Dynamic Response; Well 0, August 5

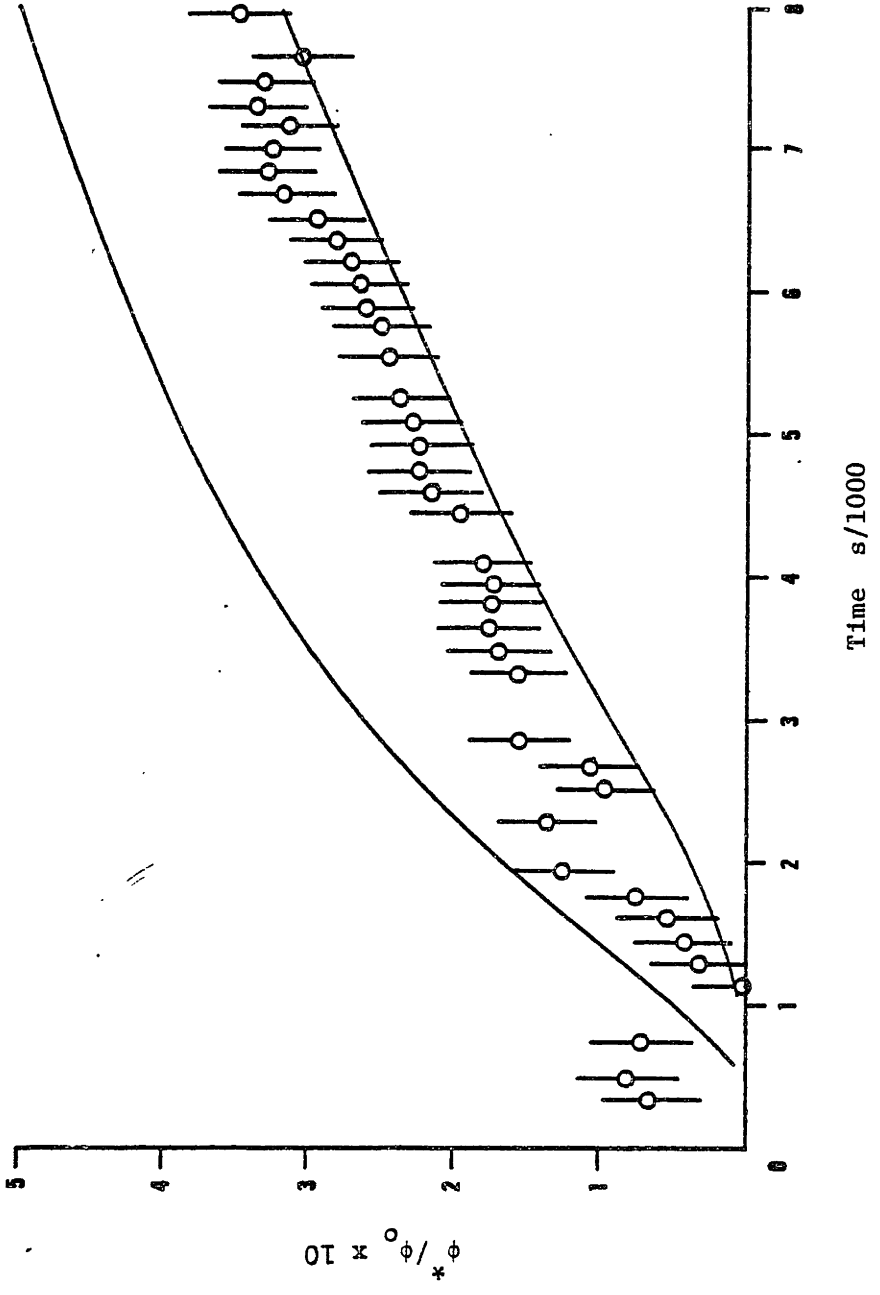

Figure 3.10 Dynamic Response; Well 4, August 5

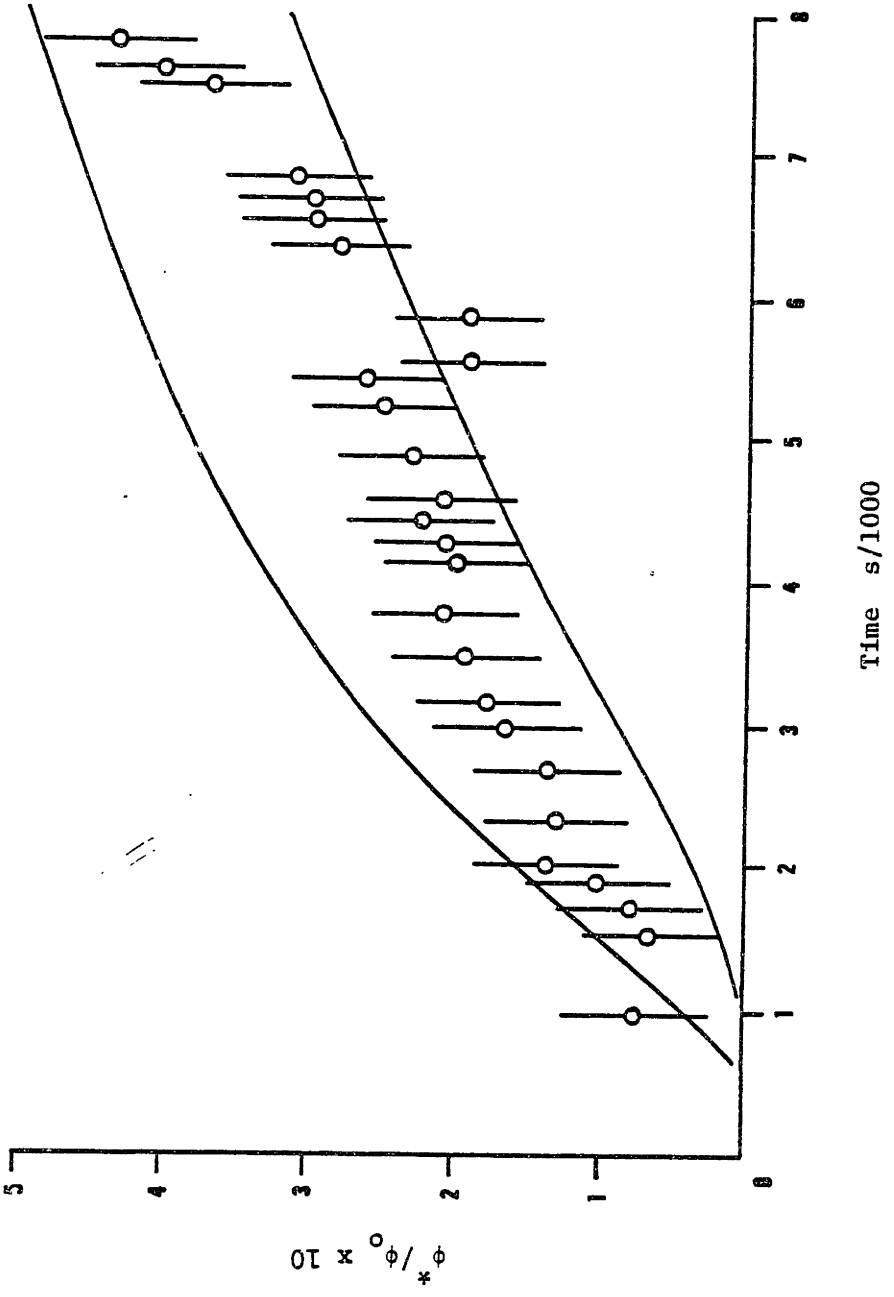

Figure 3.11 Dynamic Response; Well 8, August 5

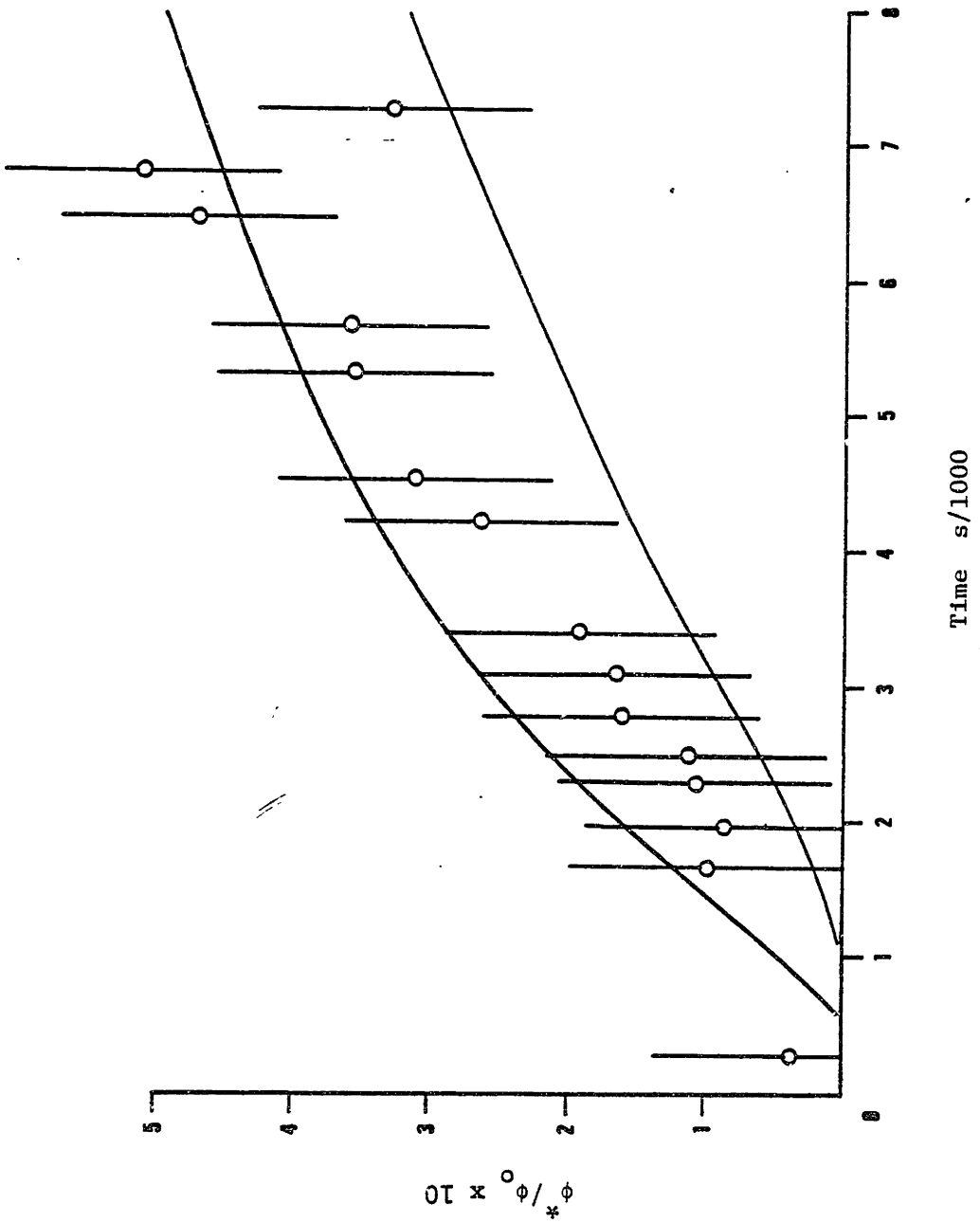

Figure 3.12 Dynamic Response; Well 0, August 6

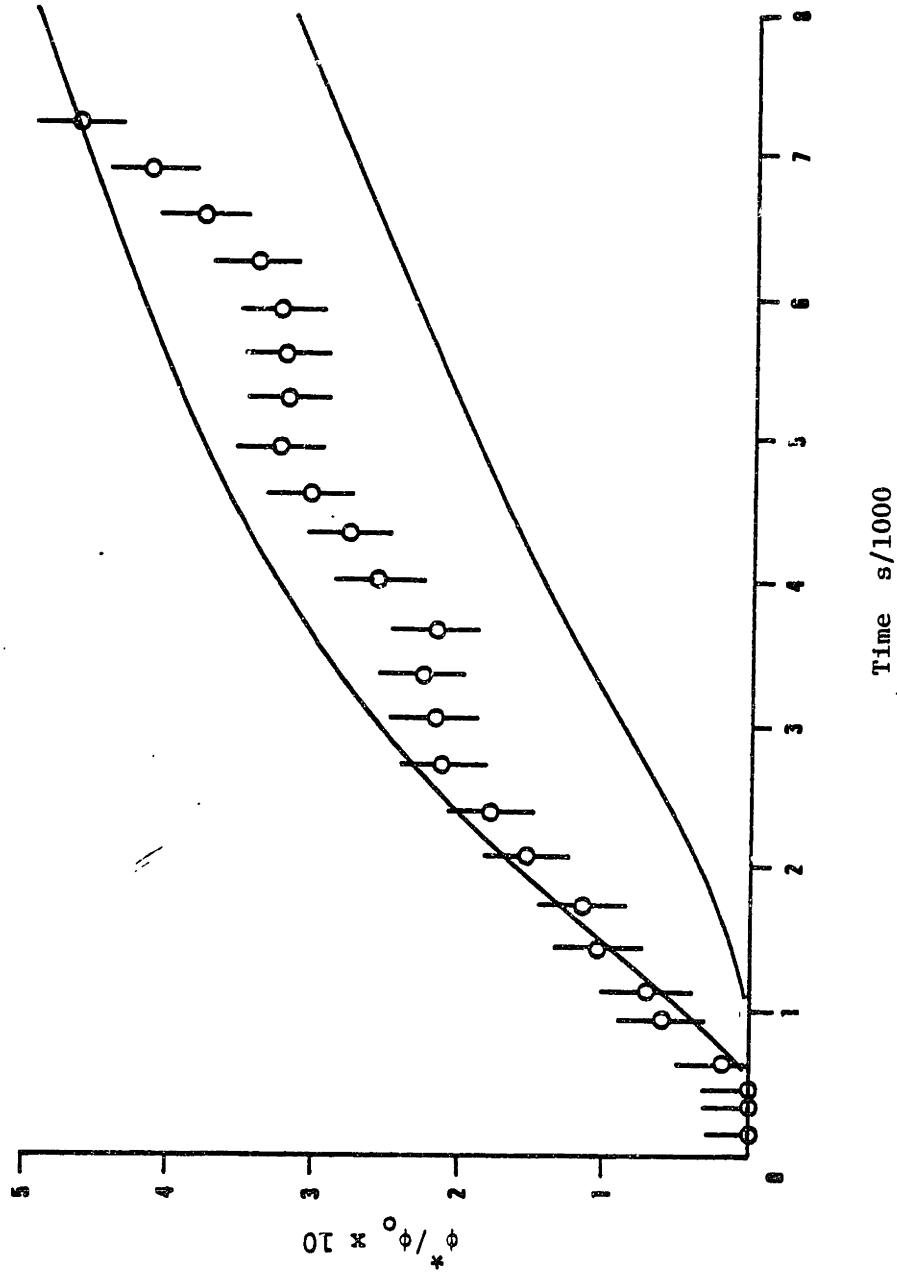

Figure 3.13 Dynamic Response; Well 4, August 6

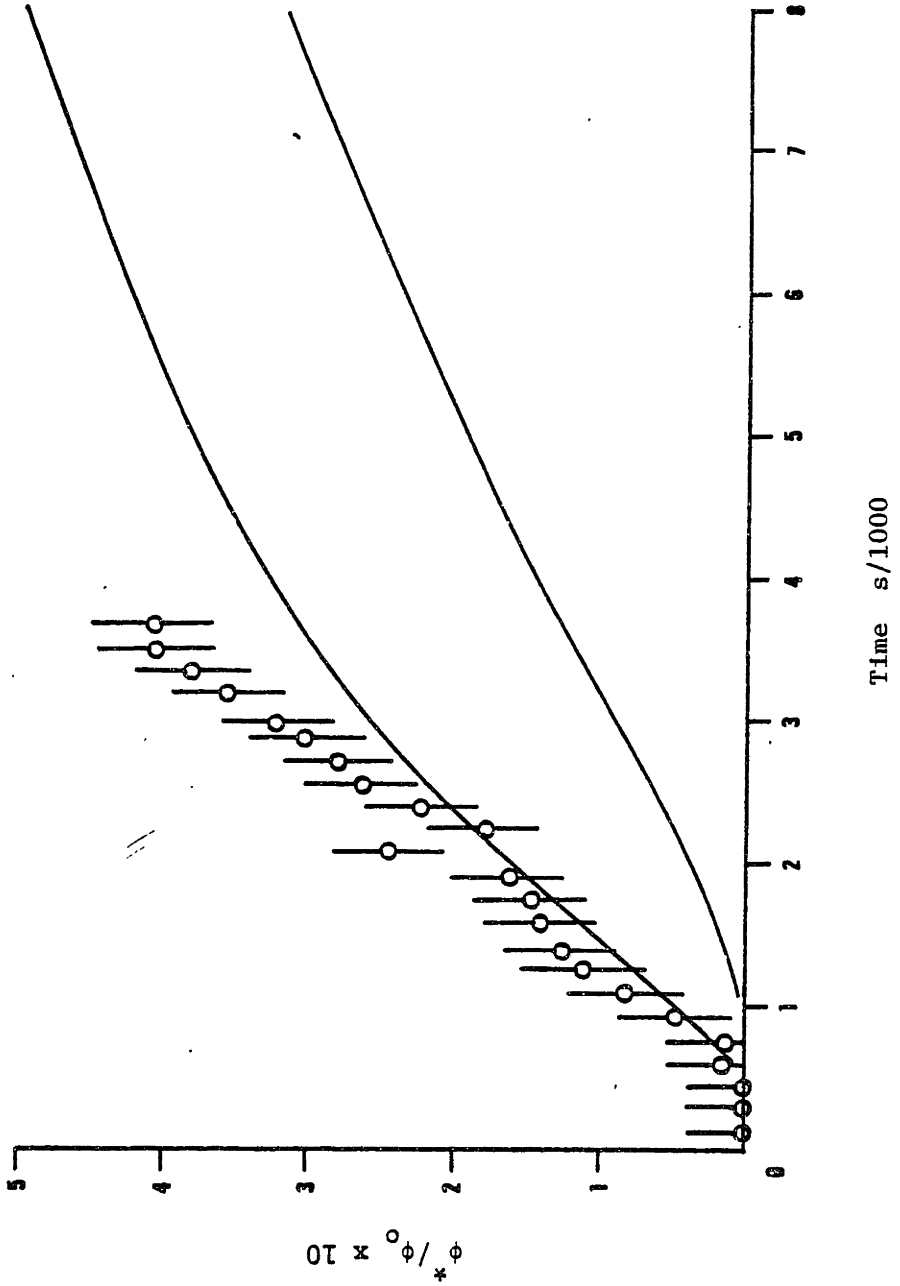

at the time of inundation and the dynamic potential ϕ^* has been normalized by the driving potential ϕ_o. The surface above well 8 was not flooded sufficiently on August 6 to obtain a good data set. The error bars on the data reflect a possible error of ±.5cm in the estimation of the ponding depth. The volume of infiltrated water contributes to the static response, but its contribution was ignored in the data reduction. The volume of infiltration is small (<.5 cm), so neglecting it introduces an error no larger than that represented by the error bars shown.

The driving potential ϕ_o can be estimated from the piezometer readings and the depths of the piezometers are known, so the parameter α can be estimated by fitting the theoretical response, equation 3.5, to the measured response. The theoretical response is defined at a point in the peat, but the measured response is averaged over the 15 cm screened depth. Therefore, the theoretical response is best represented as a range defined by the predicted response at the top and bottom of the screened interval. The theoretical range of response was fit to all five measured responses by assuming an average peat depth. The best fit is obtained by $\alpha = 0.12$, and the corresponding theoretical range is shown with the observed response as solid curves. The value of α obtained by calibration is within the range of α's defined by the interval of mean log K plus and minus a standard deviation. The ability of the theory to fit the observed data with α in the range of laboratory measurements supports the hypothetical mechanism for infiltration.

The theoretical response of the dynamic potential to infiltration by flooding can be used with Darcy's Law to predict water fluxes in the peat during infiltration. The water flux across the surface $x = 0$ of a uniform peat deposit with finite depth L is given by:

$$q_o(t) = \frac{\phi_o K}{\sqrt{\pi \alpha t}} \left\{ 1 - \mathrm{EXP}\left(\frac{-L^2}{\alpha t} \right) \right\} \qquad [3.6]$$

The cummulative volume of infiltrated water can be found by integration. The total volume of infiltration at time t after inundation is:

$$I(t) = \frac{2\phi_o K t^{1/2}}{\sqrt{\pi \alpha}} \left\{ 1 - e^{-\eta} + \sqrt{\eta \pi}\ \mathrm{ERFC}\ (\sqrt{\eta}) \right\} \qquad [3.7]$$

where $\eta = \frac{L^2}{\alpha t}$.

A value for α has been determined by fitting the theoretical dynamic potential response to observed responses at the piezometer stations in the 1981 piezometer transect. The logarithm of hydraulic conductivity is observed to be highly correlated with the logarithm of α, so equation 3.4 can be used to estimate the hydraulic conductivity of the peat given the estimated value of α. The driving potential ϕ_o has been obtained from the 1981 transect data for each observed infiltration event, so equation 3.7 can be used to estimate the volume fo infiltration that occurred. The results are shown in table 3.2

The analytical model for infiltration is based on the assumption that the change in the amount of water stored in the peat is due entirely to the water infiltrating through the upper surface. The other components of the water balance in the peat: upwelling of groundwater, influx from the creek, and evapotranspiration, are

Table 3.2 Volumes of Infiltration - 1981 Transect

Well	Date	ϕ_o (cm)	Length of Inundation (s)	Infiltrated Volume (mm)
0	8/5	14.3	11200	4.4
	8/6	16.1	7500	4.3
4	8/5	9.0	8300	2.5
	8/6	12.4	3700	2.4
8	8/5	5.2	7250	1.1
	8/6	5.3	502	0.4

ignored because the flux of water due to infiltration dominates all other fluxes in the peat, near the surface, at the time of inundation. The major source of error in the estimation of infiltration is in the estimation of the ponding depth. The error due to ignoring other water fluxes in the peat is thought to be small and positive, so the estimates of infiltrated volume may be biased upward.

4.0 A Conceptual Model of Water Movement in Peat

The flow of water in peat is fully described by Darcy's Law and the principle of conservation of mass when the stress and fluid boundary conditions and the distribution of the peat parameters K and α are known. The bases of fluid flow in a saturated porous medium have been presented in Chapter 2. A linear governing differential equation can be used if the peat properties are assumed to be constant and uniform. The observed distributions of the peat parameters K and α are presented in Chapter 3. The boundary conditions on the peat are described in the present chapter along with a few solutions of the flow equation. The resulting theoretical flow patterns are compared with observations where possible.

4.1 Uncertainty

The hydraulic conductivity of marsh peat is observed to have a three zoned structure with depth. Within each zone, the hydraulic conductivity appears to be randomly distributed. The probability distribution function for all peat in the Sippewissett Marsh is the log-normal distribution, and the mean and standard deviation are presented in table 3.1. The distribution of hydraulic conductivity within a region of peat is assumed to also be log-normal. The means and standard deviations for hydraulic conductivity inside and outside of the root zone are presented in table 3.1. The logarithm of the derived peat parameter α is highly correlated with the logarithm of hydraulic conductivity ($r = .970$) so α can be assumed to be determined for a given value of K.

The governing equation for flow that will be used in this analysis is based on the assumption that the peat parameters are constant and uniform. The variation in peat parameters from one zone to another can be represented explicitly without violating the assumption of uniformity. The random variation within zones cannot. The random nature of the peat parameters introduces uncertainty into the flow analysis.

The application of deterministic techniques to situations involving randomly varying parameters is standard procedure in problems of groundwater hydrology. The success of this approach depends on finding the "average" quantity to use in place of a random variable that results in the prediction of the most likely value of the quantity (flow rate, piezometric potential) being modeled. Freeze (1975) suggests that the hydraulic conductivity determined from the mean of log K is the appropriate "average" to use when hydraulic conductivity is randomly distributed. Therefore the hydraulic conductivity corresponding to the mean of log K and the associated value of α, found using the correlation equation 3.4, are used in this analysis to estimate the most likely characteristics of the flow regime in salt marsh peat.

The most likely value of a flow characteristic, a single number, is of limited use in understanding the subsurface flow regime in salt marshes. The variability of the value of the flow characteristic must also be represented. A range of values of the flow characteristics about the most likely value will be generated by considering a range of values of the peat parameters in the analysis. A convenient range

to use is the range defined by the values of hydraulic conductivity corresponding to the mean of log K plus and minus the standard deviation of log K. The resulting range in predicted flow characteristics represents the variability of these characteristics qualitatively, without implying anything about the probability distributions of the flow characteristics.

4.2 Description of the Subsurface Flow Problem

4.2.1 Structure of Peat

Elements of the subsurface flow problem in salt marshes are shown in figure 4.1. The three zoned peat structure observed by Hemond and Fifield (1982) and at the 1981 piezometer transect is represented. Zone 1 is the root zone, characterized by dense, light brown peat. The hydraulic conductivity corresponding to the mean of log K in the root zone is 3.1×10^{-4} cm/s. Hemond and Fifield (1982) have used a value of 9.4×10^{-5} cm/s in a numerical simulation of water movement in a one dimensional peat column. The depth of the root zone peat is 20-40 cm based on observations of color and texture in the 1981 transect cores. Zone 2 peat is separated from the root zone by a marked change in color and texture to a dark brown-black, loose structured peat. Hydraulic conductivity observed in this zone just below the root zone in the 1981 transect was about 1.8×10^{-3} cm/s. Hemond and Fifield (1982) use a hydraulic conductivity of 2.6×10^{-2} cm/s in their analysis. The depth of the zone 2 peat is controlled by the total depth of the peat and the characterization of zone 3. The change in peat properties from zone 2 to zone 3 is not as marked as between zone 1 and zone 2. Zone 3 peat is recognized as

Figure 4.1 Definition of the Flow Problem

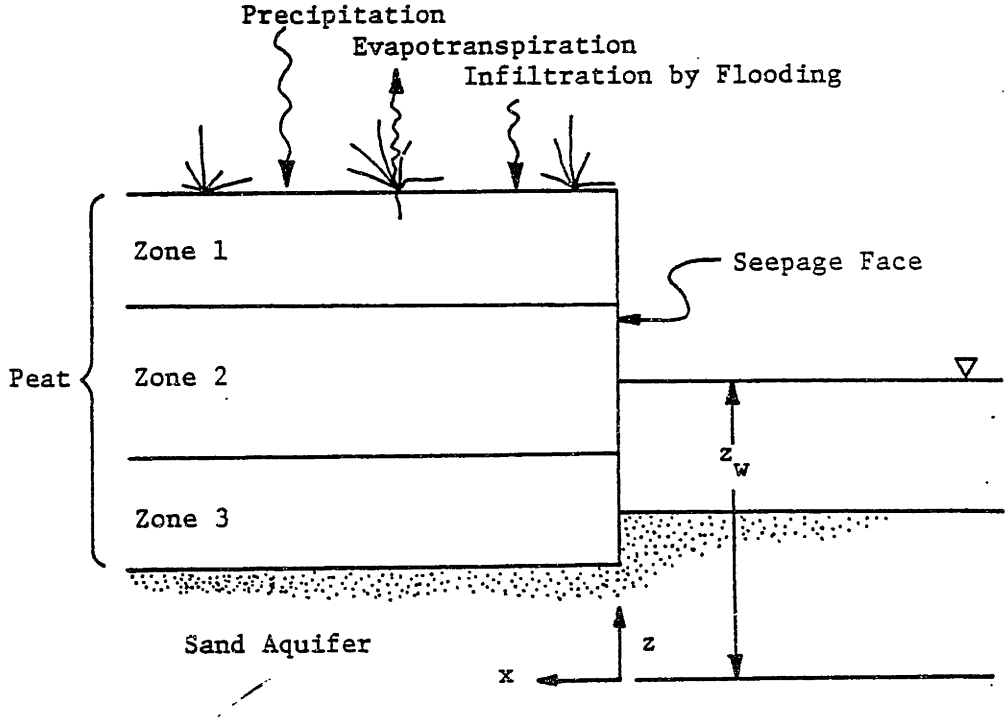

being less permeable than zone 2 peat, but due to the random distribution of hydraulic conductivity the location of the boundary between zones is open to interpretation. The role that zone 3 plays in the subsurface flow regime is to control the degree of connection of the water in the peat to the water in the underlying sand aquifer. Hemond and Fifield (1982) use a 30 cm thick layer of peat with hydraulic conductivity of 1.8×10^{-5} cm/s. The clay layer (~ 20 cm thick, $K = 7 \times 10^{-6}$ cm/s) can be considered as the zone 3 material at the 1981 piezometer transect (see figure 3.5).

An outwash deposit of coarse sand and gravel underlies the coastal area at the Sippewissett Marsh. This is a freshwater aquifer and well records in the area show it extending to depths of at least 100 feet (D. LeBlanc, USGS, personal communication). The sand aquifer potential is represented as a boundary condition in this analysis.

4.2.2 Lower Boundary Condition

The piezometric potential in the sand aquifer is a function of time as a result of its connection with the ocean. The piezometric potential at the sand-peat interface can be represented by a Fourier series:

$$\phi(t) = \phi_s + y_1\cos(w_1 t + \varepsilon_1) + y_2\cos(w_2 t + \varepsilon_2) + \ldots \qquad [4.1]$$

The depth and high conductivity of the sand aquifer buffer the potential ϕ_s from the effects of the relatively small exchange of water expected across the sand-peat interface. Therefore the boundary condition at the sand-peat interface for the flow of water in the peat is a time dependent potential given by equation 4.1. The time averaged potential ϕ_s can be considered uniform on the peat-sand

interface for the purposes of this analysis. The tidal period (T = 12.5 hours) is the period of primary interest in the variation of the potential in the sand. The amplitude of the variation of ϕ_s at this period is ~10 cm where it has been measured in the Sippewissett marsh.

4.2.3 Creek Bank Boundary Condition

The boundary condition on the flow problem at the creek bank is a mixture of three different boundary conditions. Where the peat face is submerged, the boundary condition is a constant potential controlled by the vertical pressure distribution in the creek. Since this is hydrostatic, the applied potential is the same everywhere below the water level and is simply equal to the elevation of the water surface. Above the water surface, the pore pressures are controlled by the interface with the atmosphere. Here the pore pressures at the surface are zero everywhere and the potential is simply equal to the elevation of the point of interest. Some distance above the creek level, the pore pressures within the peat may be less than atmospheric. Following the assumption of full saturation, the boundary condition is a zero flux boundary controlled by capillary forces at the surface. Negative pore pressures may well be limited to the root zone, the upper 20-40 cm of peat. The vertical boundary condition on the root zone is relatively unimportant because the flow of water is predominantly vertical there. So for purposes of discussion, the creek bank boundary condition will be described as an applied potential boundary defined by:

$$\phi(z,t) = z_w(t) \qquad z < z_w(t)$$
$$\phi(z,t) = z \qquad z \geq z_w(t) \qquad [4.2]$$

where z_w is the elevation of the water surface in the creek.

The elevation of the water surface in the creek varies in response to the effects of tides, storm surges and seiching of the coastal water body as modified by the dynamics of flow in the creeks. The creek elevation can be described by a Fourier series as was the potential in the sand aquifer.

$$z_w(t) = z_o + z_1\cos(w_1 t + \varepsilon_1) + z_2\cos(w_2 t + \varepsilon_2) + \ldots \quad [4.3]$$

The amplitude of the observed tidal fluctuations is 40 cm.

The simplified creek bank boundary condition is fully described by equations 4.2; however, intuition is not aided by this description. Further simplification and time averaging enable a graphical representation of the distribution of the piezometric potential on the creek bank. If only the variation of the creek level at the tidal period is considered, then the time averaged potential at a point in the range of tides is given by:

$$\overline{\phi}(z) = \frac{1}{T}\left\{ 2\int_o^{t_1} \frac{H}{2}(1 + \cos \omega t)dt + z(T - 2t_1)\right\} \quad [4.4]$$

where H is defined in figure 4.2 and t_1 is half of the period of inundation per tidal cycle at height z:

$$t_1 = \frac{T}{2\pi}\cos^{-1}\left(\frac{2z}{H} - 1 \right)$$

The time averaged potential above the range of tides is z, and the averaged potential below the range of tides is z_o. The variation in the average potential over the entire creek bank is sketched in figure

4.3, and the variation in averaged potential through the range of tides, obtained from equation 4.4, is shown in figure 4.4. The averaged potential increases with decreasing frequency of inundation. This will induce vertical movement of water just inside of the peat downward into the tidal range. The averaged potential below the tidal range is constant with depth , so no vertical movement of water is induced here by the action of the tides. Water draining into the tidal range from above will drain out of the peat within the tidal range.

4.2.4 Surface Boundary Condition

The boundary condition at the surface of the peat is controlled by three processes: precipitation, evapotranspiration, and infiltration. Precipitation is fairly evenly distributed through the year at the Sippewissett Marsh. The average monthly precipitation at the nearby Hatchville station of the National Oceanic and Atmospheric Administration is 3.64 inches. As a first approximation all precipitation is assumed to infiltrate into the peat. The resulting boundary condition due to precipitation is a prescribed surface flux of 2.9×10^{-6} cm/s. The rate of water withdrawal from the peat due to evapotranspiration is a function of plant physiology, local meteorology, solar radiation, and possibly soil water pore pressures and salinity . The nature of the relationship between these variables and evapotranspiration in the salt marsh is the subject of ongoing study. Direct measurements of evapotranspiration are scarce. Hemond and Fifield (1982) estimate evapotranspiration fluxes from 0.4 cm/day to 1.6 cm/day (4.6×10^{-6} - 1.8×10^{-5} cm/s) based on the results of an energy budget calculated

Figure 4.2 Simplified Creek Bank Boundary Condition

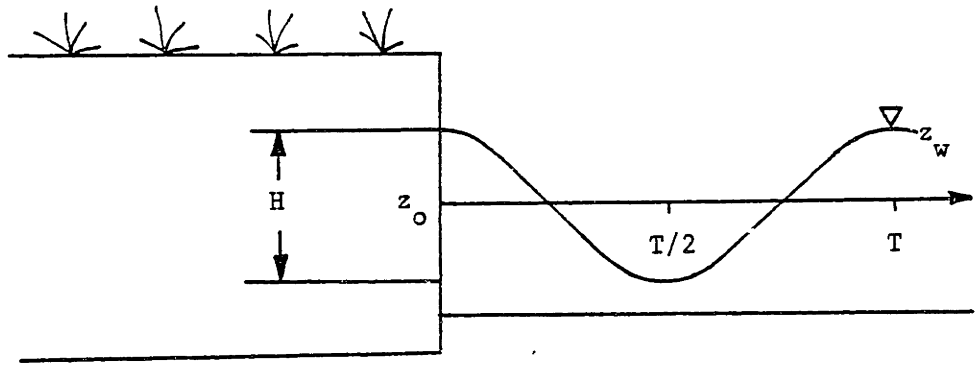

Figure 4.3 Time Averaged Boundary Potential

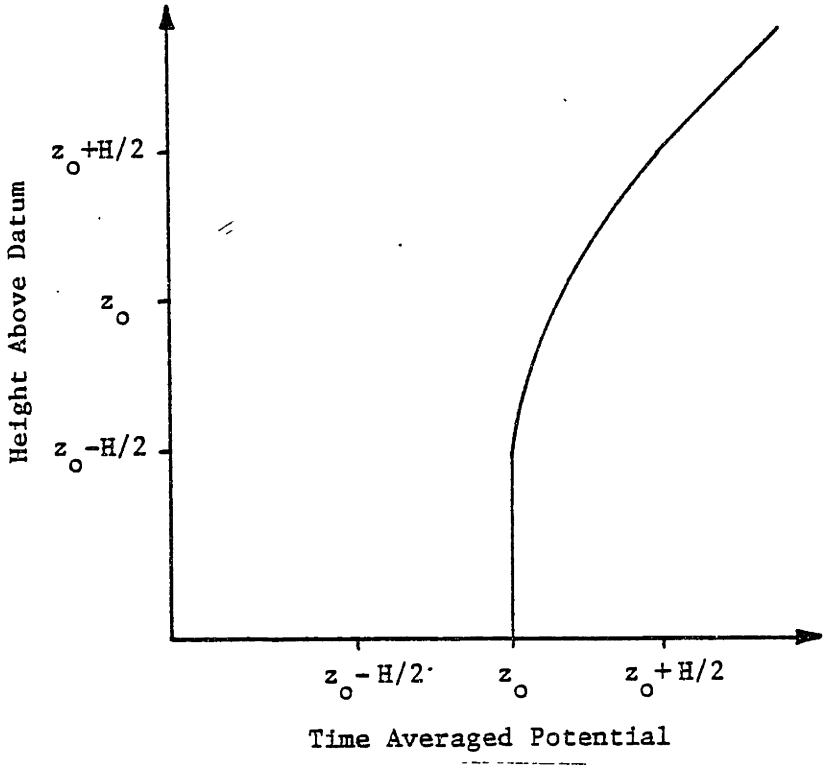

Figure 4.4 Time Averaged Potential Within the Tidal Range

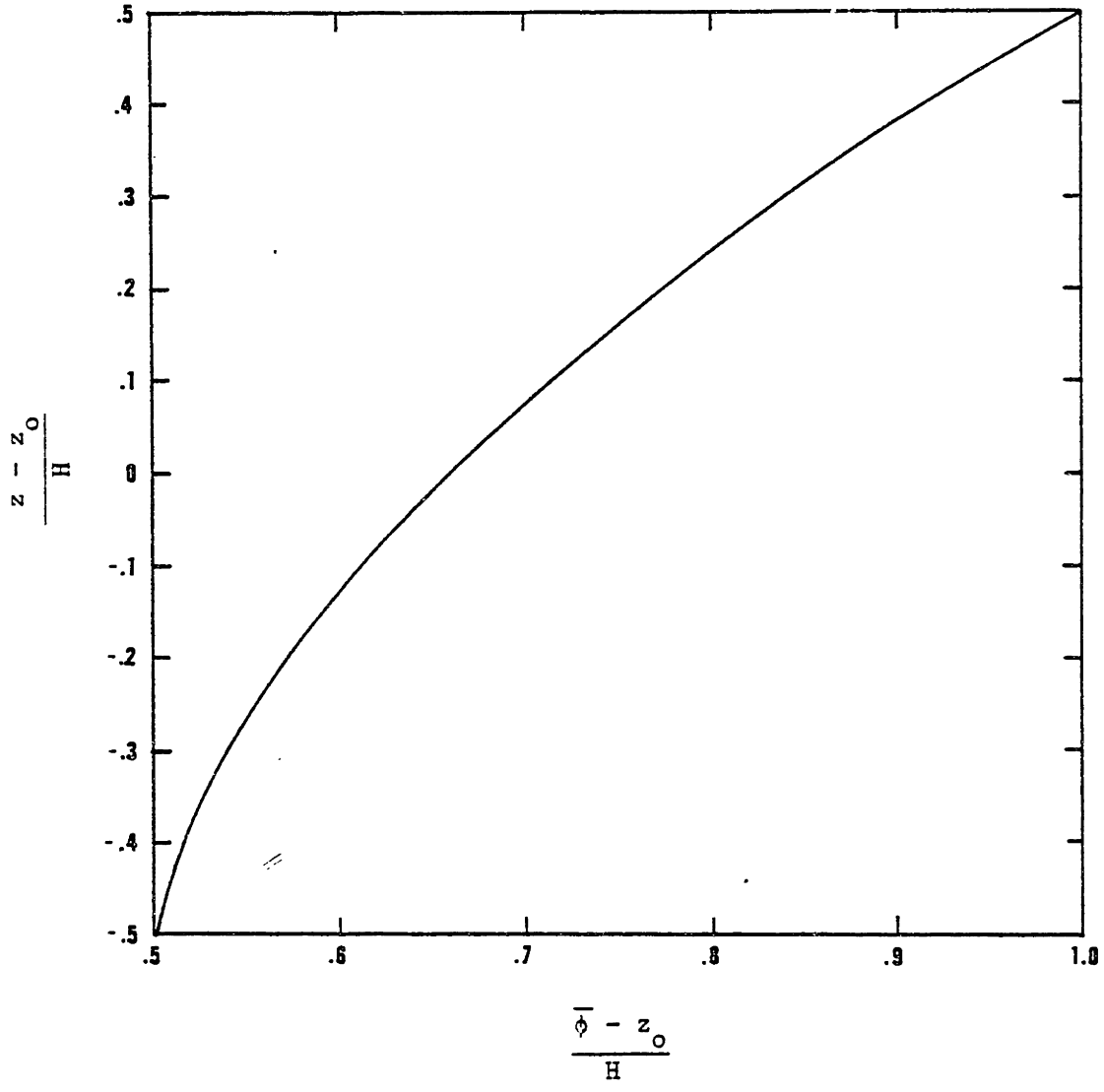

in the marsh during the growing season by Teal and Kanwisher (1970). Water is withdrawn from the peat throughout the root zone, so evapotranspiration is ideally represented as a distributed fluid sink.

Infiltration due to flooding of the peat surface can be modeled as the response to a step increase in the piezometric potential at the surface. The amount of infiltration that occurs during a given flooding event depends on the duration of flooding and the pressure drop across the pore water-atmosphere interface. It is necessary, because of lack of detailed information, to use time averaged values of precipitation and evapotranspiration. Infiltration must also be averaged to be consistent. The conditions controlling the amount of infiltration can be assumed to recur periodically at least over the short term, so the time averaged infiltration boundary condition is a surface flux dependent in some way on the averaged potentials in the peat and the frequency of flooding.

The number of flooding events per month and the duration of each flooding event vary with distance from the creek bank. The elevation of the water surface at high tide varies with the spring tide-neap tide cycle, and the marsh surface slopes downward towards the creek. Areas of the marsh near the creek bank are flooded more often and for longer periods than areas far from the creek, and the amount of infiltration is greater for areas near the creek than for areas far from the creek. This can be seen in the volumes of infiltration inferred from the 1981 transect data, table 3.2.

The potentials in the peat depend on the magnitude and distribution of evapotranspiration, precipitation, and infiltration in time. This information is unavailable for the processes of evapotranspiration and precipitation and can only be estimated at this point for infiltration. Therefore, the dependence of the average infiltration flux on averaged potential can not be considered in this analysis; the dependence of infiltration on the frequency of flooding can.

The conditions observed at the 1981 transect and the distribution of peat parameters derived from the laboratory work can be used to estimate the variation in infiltration throughout the marsh. The surface peat properties control the process of infiltration, so the range of parameters defined by the mean plus and minus the standard deviation of log K in the root zone (see table 3.1) are appropriate. The result of these calculations is shown in table 4.1. Notice that the range of infiltration values in table 4.1 brackets the values inferred from the 1981 transect observations. The computed volumes are also consistent with the observed values of infiltration, in which the observed range was 0-20 mm with most observations less than 5 mm (Burke et al, unpublished; Hemond and Burke, 1981)

The values of infiltrated volume in table 4.1 were estimated using conditions observed during two flooding events on two consecutive days. Two other flooding events occurred on these days but were not observed because they occurred at night. The marsh surface was flooding because the period of observation coincided with the spring tides. The high tide first observed was higher than the second. A

Table 4.1 Distribution of Infiltration

Distance From Creek cm	ϕ_o cm	Time of Inundation s	Infiltrated Volume $K = 2 \times 10^{-3}$ mm	$K = 3 \times 10^{-4}$ mm	$K = 5 \times 10^{-5}$ mm
100	14.3	10000	15.9	9.7	3.0
	16.1	7500	16.6	9.3	3.1
500	9.0	8300	9.6	5.6	1.7
	12.4	3680	10.7	5.1	1.6
900	5.2	7240	5.4	3.0	0.9
	5.3	500	1.9	0.8	0.3

week later, during neap tides, the water level in the creek at high tide was not high enough to flood the marsh. Spring tides, and thus the surface infiltration events, have a period of about 14 days.

The magnitude and spatial distribution of the time averaged infiltration flux were estimated from the available information in the following manner. Several amounts of infiltration occurring over a typical spring tide cycle were estimated at each distance from the creek from the estimated per event infiltration volumes shown in table 4.1. Amounts of infiltration per spring tide cycle were estimated from the two observed events using reasonable but arbitrary distributions. The volumes obtained from the mean log K in the root zone were used to get the best estimate of infiltration. The data, several 14 day volumes at each of three distances from the creek, were fitted with an exponential function relating the average infiltration flux to distance from the creek. The exponential form was chosen solely on the basis of convenience, recognizing the nature of the data involved. The resulting relation for the infiltration flux boundary condition is:

$$I(x) = (9.8 \times 10^{-6})e^{-.0022x} \text{ cm/s} \qquad [4.5]$$

where x is the distance in centimeters from the creek.

The boundary conditions on the subsurface flow problem in the salt marsh are summarized in table 4.2. The approximate nature of these formulations is the result of the tradeoff between the desire to be as complete as possible in the statement of the problem on one hand and a lack of information on the other.

Table 4.2 Summary of Boundary Conditions

Boundary	Mathematical Description	
Sand Interface	$\phi(t) = \phi_s + 10 \cos(1.4 \times 10^{-4} t + \varepsilon)$	cm
Creek Bank	$\phi(z,t) = z_w(t) \quad z < z_w(t)$	cm
	$\phi(z,t) = z \quad z \geq z_w(t)$	
	$z_w(t) = z_o + 40 \cos(1.4 \times 10^{-4} t + \varepsilon)$	
Peat Surface	$\bar{q}(x) = P - ET + I(x)$	cm/s
	$P = 2.9 \times 10^{-6}$	
	$ET = 4.6 \times 10^{-6} - 1.8 \times 10^{-5}$	
	$I(x) = 9.8 \times 10^{-6} \ EXP(-.002x)$	

4.3 Response to Dynamic Forcing

The boundary conditions on the subsurface flow problem in salt marsh peat are determined by the effects of dynamic processes in the salt marsh. In deriving a mathematical description of the boundary conditions in the previous section, it has been necessary to simplify the representation of the dynamic processes because of lack of information. The processes of infiltration due to precipitation and flooding and evapotranspiration are represented as time averaged steady state fluxes. Representation of the dynamic components of the creek bank boundary condition and the peat-sand interface is limited to the component at the tidal frequency. Not enough information is available to estimate the significant variations at lower frequencies, and it will be seen that variations at higher frequencies have little effect on the movement of water in the peat. The steady state and dynamic components of the boundary lead to steady state and dynamic flow patterns in the peat. The linearity of the governing equation, equation 2.8, permits the separate solution for the steady state and dynamic components of the flow.

Further simplification of the creek bank boundary condition at this point will simplify the analysis. Quantitative description of the flow of water in peat has already been compromised by 1) the random distribution of peat parameters, and 2) the approximation already present in the statement of the boundary conditions. The approximation proposed will allow a simple qualitative description of the flow regime, and its effect on the quantitative results can be assessed by a comparison to the range of observed fluxes across the creek bank.

The creek bank boundary condition is complicated by the moving water surface in the creek. Below the water surface the boundary condition is a prescribed potential that follows the variation in the creek level. Above the water surface the boundary condition is a constant potential equal to the elevation of the point considered. The variation of the potential at a point within the tidal range on the boundary resembles a clipped sine wave. The variation of the potential at a point below the tidal range follows the creek elevation exactly. The deviation of the variation in the prescribed potential from the variation in the creek level is small in the lower reaches of the tidal range as can be seen in figure 4.4. The simplification that will be made here is to say that the variation of the depth averaged potential on the creek bank is sufficiently well described by the variation in the creek level.

$$\bar{\phi}(x,t) = 40 \cos (1.4 \times 10^{-4} t + \varepsilon) \quad x = 0 \qquad [4.6]$$

This approximation is made for convenience, but some sort of approximation is necessary because the location of the tidal interval relative to the peat face is unspecified.

The solution of the governing equation for the case of a sinusoidal boundary potential is given in the appendix. The quasi-steady state variation of the depth averaged potential is given by:

$$\bar{\phi}(x,t) = \phi_o \mathrm{EXP}\left(-\sqrt{\frac{\omega}{2\alpha}}\, x \right) \cos\left(\omega t - \sqrt{\frac{\omega}{2\alpha}}\, x + \varepsilon \right) \qquad [4.7]$$

where ϕ_o is the amplitude of the variation of the potential on the surface. The depth averaged fluxes in the peat are given by:

$$\bar{q}(x,t) = K\phi_o \sqrt{\frac{\omega}{\alpha}}\, \mathrm{EXP}\left(-\sqrt{\frac{\omega}{2\alpha}}\, x \right) \cos\left(\omega t - \sqrt{\frac{\omega}{2\alpha}}\, x + \frac{\pi}{4} + \varepsilon \right) \qquad [4.8]$$

Fluxes lead the potential by T/8. Notice that both the variation in potential and the flux due to periodic forcing at the peat boundary are attenuated exponentially with distance from the boundary. Also the degree of attenuation is greater for higher frequencies and lower values of α (lower hydraulic conductivity).

If full attenuation is defined as a 95 percent reduction in amplitude and zero attenuation as a 5 percent or less reduction in amplitude, a functional relationship exists between the distance to full (zero) attenuation of the effects of the variation in potential on the boundary and the frequency of the variation. These relationships are shown in figures 4.5 and 4.6 for a range of peat parameters. The effects of periodic boundary forcing at the tidal period are fully attenuated ten meters from the creek bank in most cases. The effects of periodic forcing at the frequency of the spring tides carry three times as far.

Equation 4.8 can be integrated to find the volume of water exchanged across the creek bank, that is the total volume of infiltration or exfiltration that takes place between flow reversals. The volume of exchange is :

$$V_s = \frac{2\,\phi_o\,K}{\sqrt{(\omega\alpha)}} \qquad [4.9]$$

also a function of the frequency of the boundary potential. The relation between the normalized exchange volume V_s/ϕ_o and the frequency of the boundary potential variation is shown in figure 4.7 for a range of peat parameters. The amplitude of the tidal forcing is 40 cm,

Figure 4.5 Distance to 95% Attenuation

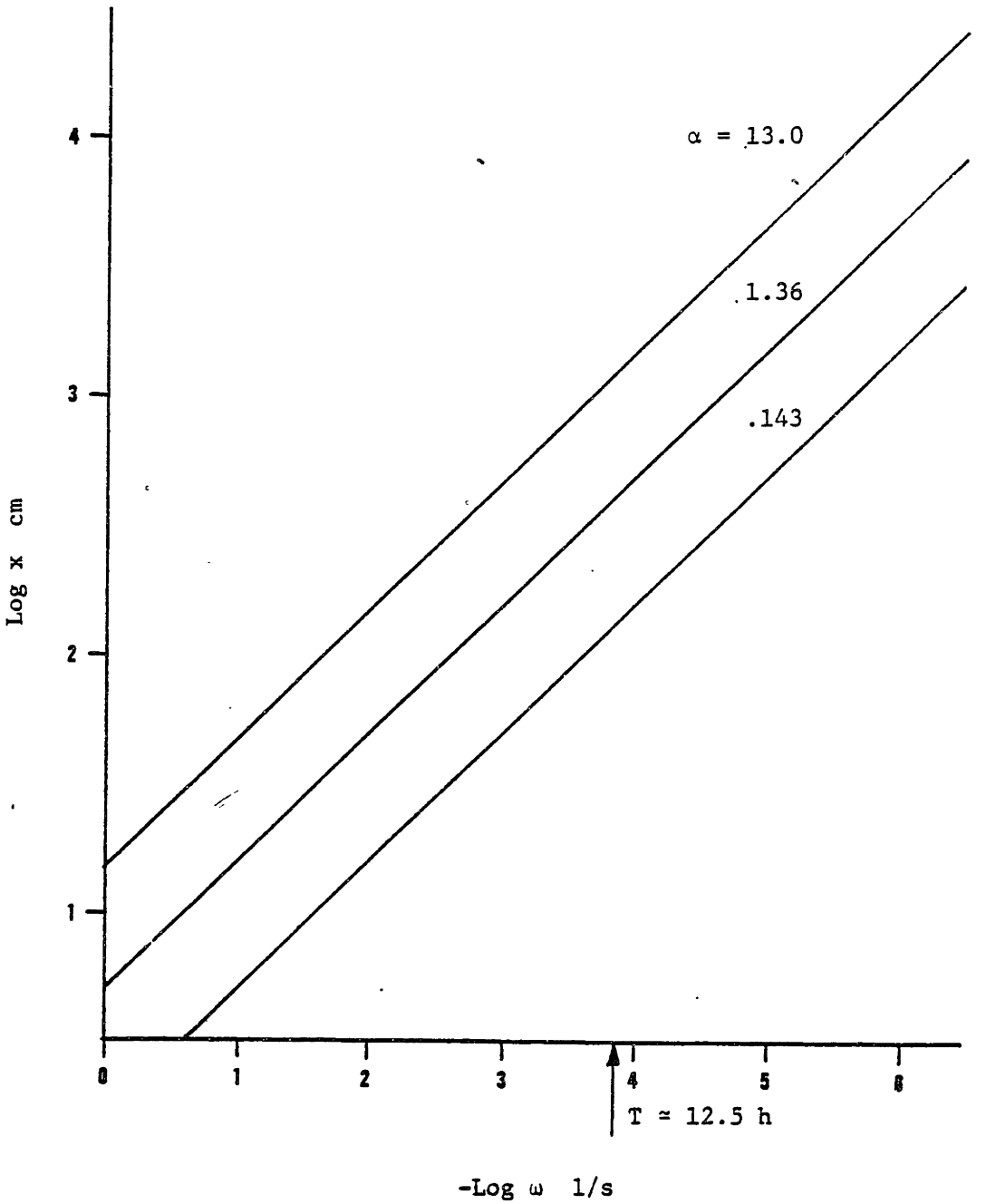

Figure 4.6 Distance to 5% Attenuation

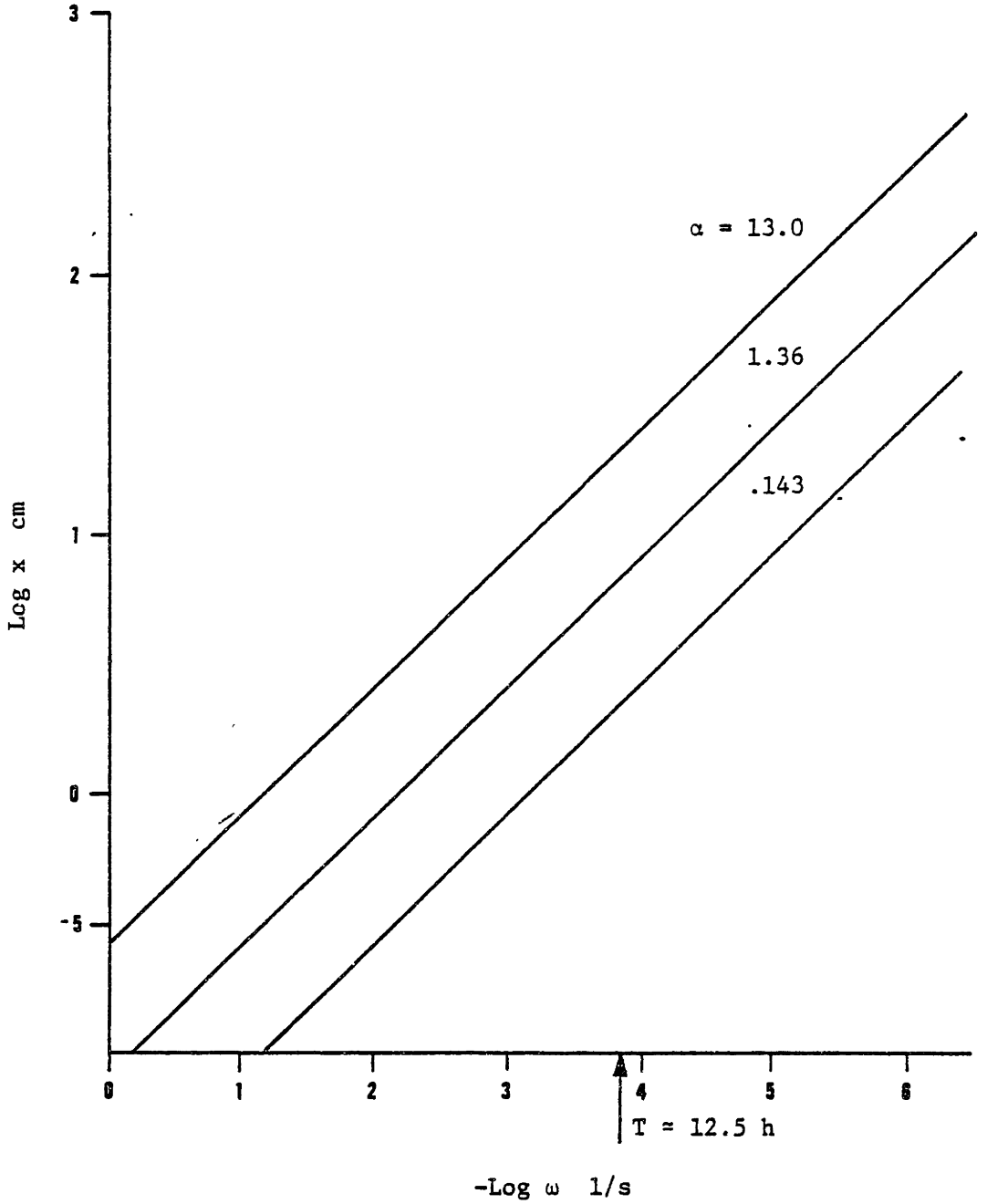

Figure 4.7 Exchange Volume

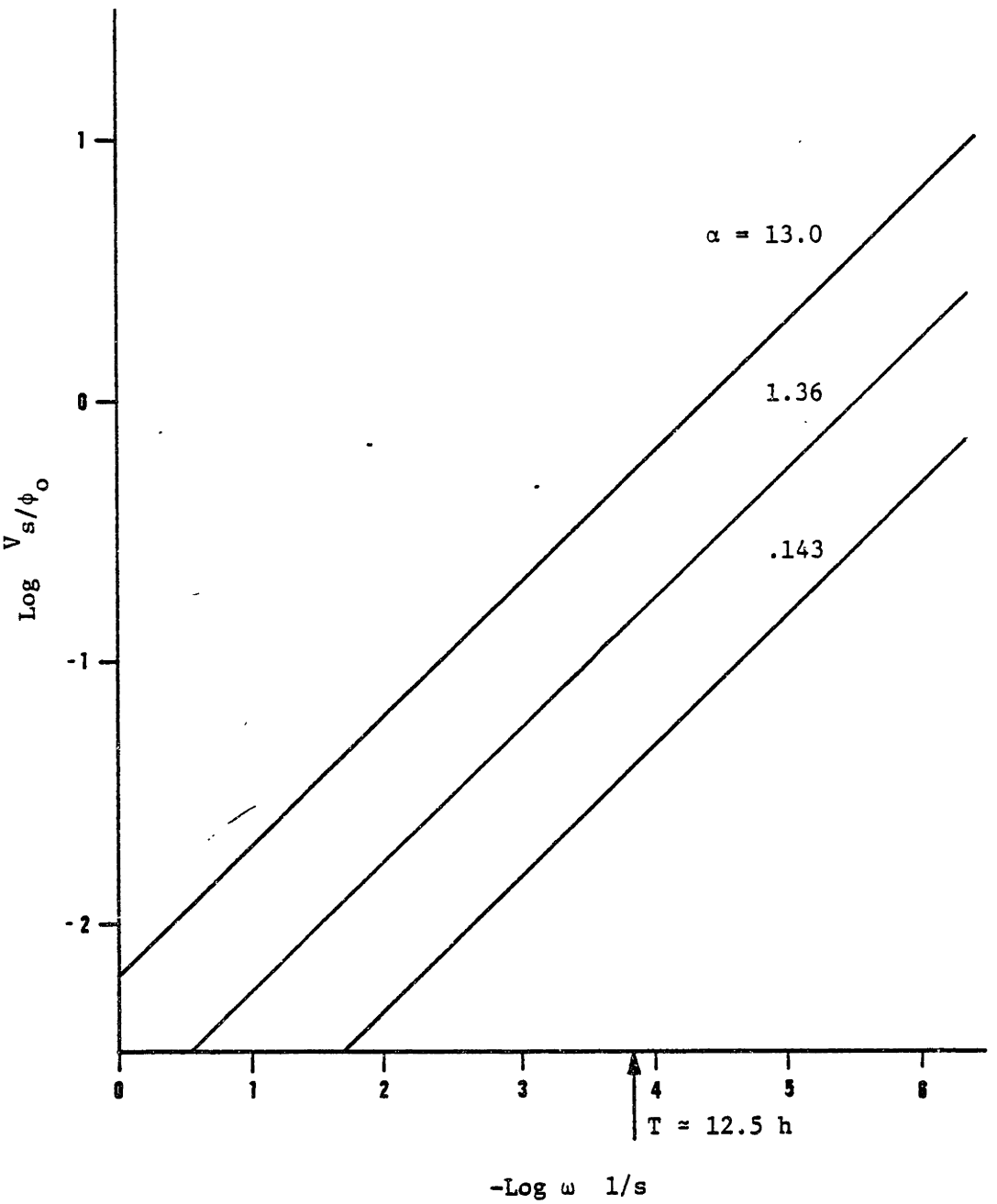

and the range of exchanged volumes at the tidal frequency is 1.25 cm to 23 cm with 6 cm the most likely value. This compares well with the 4-10 cm range of exchange volumes suggested by the field observations (Fifield, personal communication). The degree of agreement between the theoretical range of exchange volumes and the observed volumes supports the use of the approximation to the creek bank boundary condition at this level of analysis.

Effects due to periodic variation in the potential at the peat-sand interface are expected to be more highly attenuated than the creek bank effects owing to the presence of the zone 3 peat at the boundary (lower α). The high attenuation combined with the low amplitude (10 cm) of the variation in potential suggests that the effect of the dynamic component of this boundary condition on the flow in the peat will be small. This has been observed to be the case in numerical simulations by Hemond and Fifield (1982). The volume periodically exchanged across the peat-sand boundary is estimated to be on the order of tenths of centimeters.

4.4 Steady State Solutions

The dynamic flow patterns are superimposed on a steady flow pattern determined by the time averaged components of the boundary conditions. The three zone structure of peat will make it possible to describe the general nature of the two dimensional flow pattern using a one dimensional water balance model. The case of a permeable soil bounded by less permeable deposits is known as a "leaky aquifer" in groundwater hydrology. A simple solution for flow in the leaky

aquifer can be obtained by observing that horizontal flow takes place in the permeable layer while the flow in the less permeable layers is generally vertical (Bear, 1979).

The differential equation governing the long term horizontal flow of water in the permeable layer of peat can be formulated from a mass balance on a differential slice of peat, figure 4.8. The horizontal flow rate is determined by Darcy's Law applied to the depth averaged potential $\bar{\phi}$ in the permeable layer. The boundary condition at the creek bank is a prescribed potential equal to the mean creek level. The piezometric potential is defined as the sum of a pressure head and the distance from an arbitrary datum. It is convenient here to choose the datum in such a way that the prescribed potential at the creek bank is zero. The flow of water into the permeable layer from above is determined by the balance between the water fluxes at the peat surface.

$$q_1 = P - ET + I_o\, e^{-\gamma x} \qquad [4.10]$$

The exchange of water between the permeable peat layer and the underlying sand aquifer is determined by the difference in piezometric potential and the thickness and hydraulic conductivity of the lower layer of less permeable peat.

$$q_2 = K_3[\phi_s - \phi(x)]/H_3 \qquad [4.11]$$

The water balance at steady state leads to a differential equation in terms of the depth averaged potential in the permeable layer.

$$H_2K_2\partial^2\bar{\phi}/\partial x^2 = -(q_1 + q_2) \qquad [4.12]$$

Figure 4.8 Water Balance on a Slice of Peat

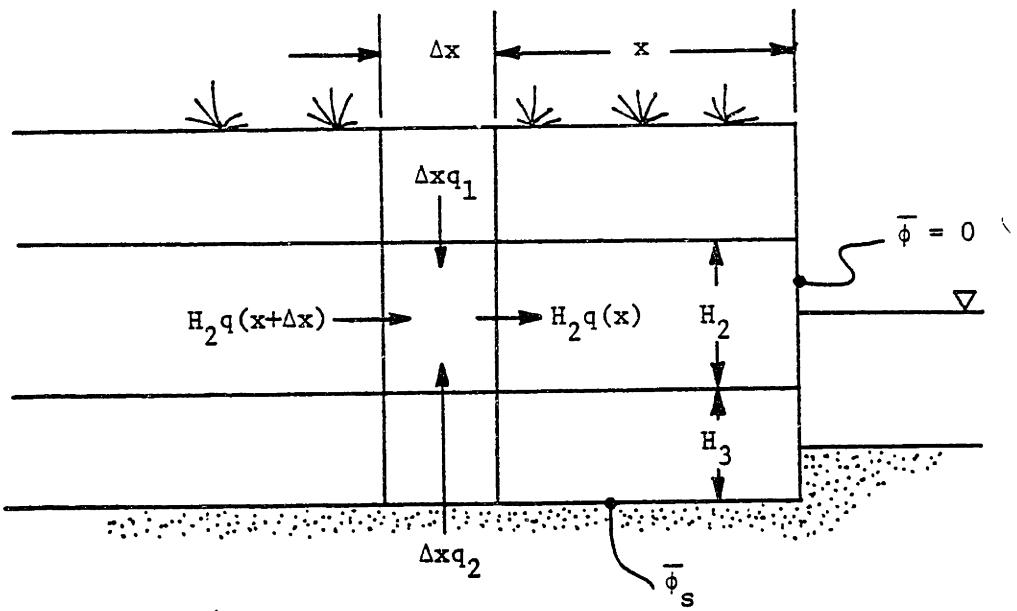

Substituting from equations 4.10 and 4.11, the following equation is obtained,

$$H_2K_2\frac{\partial^2\overline{\phi}}{\partial x^2} - \frac{K_3}{H_3}\overline{\phi} = ET - P - \frac{K_3}{H_3}\phi_s - I_o e^{-\gamma x} \qquad [4.13]$$

The boundary conditions are:

$$\begin{aligned} &\overline{\phi}(x) = 0 && x = 0 \\ &\partial\overline{\phi}/\partial x = 0 && x \to \infty \end{aligned} \qquad [4.14]$$

The solution to equation 4.13 is derived in the appendix.

$$\overline{\phi}(x) = \left[\frac{C}{B} - \frac{D/A}{(\gamma^2 - B/A)}\right] e^{-\sqrt{xB/A}} + \frac{D/A}{(\gamma^2 - B/A)} e^{-\gamma x} - \frac{C}{B}$$

$$A = H_2K_2$$

$$B = K_3/H_3 \qquad [4.15]$$

$$C = ET - P - K_3/H_3\ \phi_s$$

$$D = -I_o$$

Equation 4.15 along with equations 4.10 and 4.11 specify the flow rates everywhere in the simplified steady flow regime. The flow field equations are useful as a means of visualizing the flow of water in the peat under various specified conditions. The flow field depends on nine parameters, and each parameter contains a degree of uncertainty. Therefore, the flow field equations are useless as a tool for parameter estimation.

The parameters for six flow cases to be investigated are presented in table 4.3. The values of the parameters relating to the water balance in the root zone are the best estimates of these parameters

Table 4.3 Water Balance Case Descriptions

Case	P ($\times 10^6$)	ET ($\times 10^6$)	I_o ($\times 10^5$)	γ	K_2 ($\times 10^3$)	H_2	K_3 ($\times 10^5$)	H_3	ϕ_s
1	3.0	7.0	1.0	.0022	2.0	50	2.0	30	20
2	3.0	7.0	1.0	.0022	1.0	50	2.0	30	20
3	3.0	7.0	1.0	.0022	2.0	50	0.7	30	20
4	3.0	7.0	2.0	.0022	2.0	50	2.0	30	20
5	3.0	7.0	0.0	.0022	2.0	50	2.0	30	20
6	3.0	0.0	1.0	.0022	2.0	50	2.0	30	20

1) Base Case
2) K_2 Sensitivity
3) K_3 Sensitivity
4) Peak Infiltration
5) Zero Infiltration
6) Zero Evapotranspiration

as presented in section 4.2. The water balance in the root zone varies with distance from the creek as shown in figure 4.9. The depths of the second and third zones of peat were chosen to approximate the geometry at the 1981 transect. The value of the potential at the peat-sand interface was chosen on the basis of piezometer observations in the marsh. The hydraulic conductivity of the permeable zone was chosen to match the hydraulic conductivity observed beneath the root zone at the 1981 transect. Fifield (1981) found peat directly in contact with the sand aquifer in the majority of the cores taken in the Sippewisset Marsh, so the hydraulic conductivity for the lower less permeable zone K_3 was taken from the value for zone 3 peat used by Hemond and Fifield (1982). Hemond and Fifield (1982) use a higher hydraulic conductivity in the permeable zone than that adopted for the base case here, so case 2 demonstrates a higher hydraulic conductivity in zone 2. Clay serves as the lower permeability material at the peat-sand boundary at the 1981 transect, so case 3 is presented using the hydraulic conductivity of clay in zone 3.

Three of the flow field cases have been designed to crudely simulate the variation of infiltration by flooding and of evapotranspiration in time. Infiltration occurs during periods of spring tides; during neap tides the infiltration is zero. This has been simulated by doubling the time averaged rate of infiltration in case 4 (spring tide) and setting the rate of infiltration to zero in case 5 (neap tide). Evapotranspiration shows a seasonal variation. The value of evapotranspiration used here was estimated during the growing season. In winter and early spring the evapotranspiration is

Figure 4.9 Input From Water Balance in the Root Zone

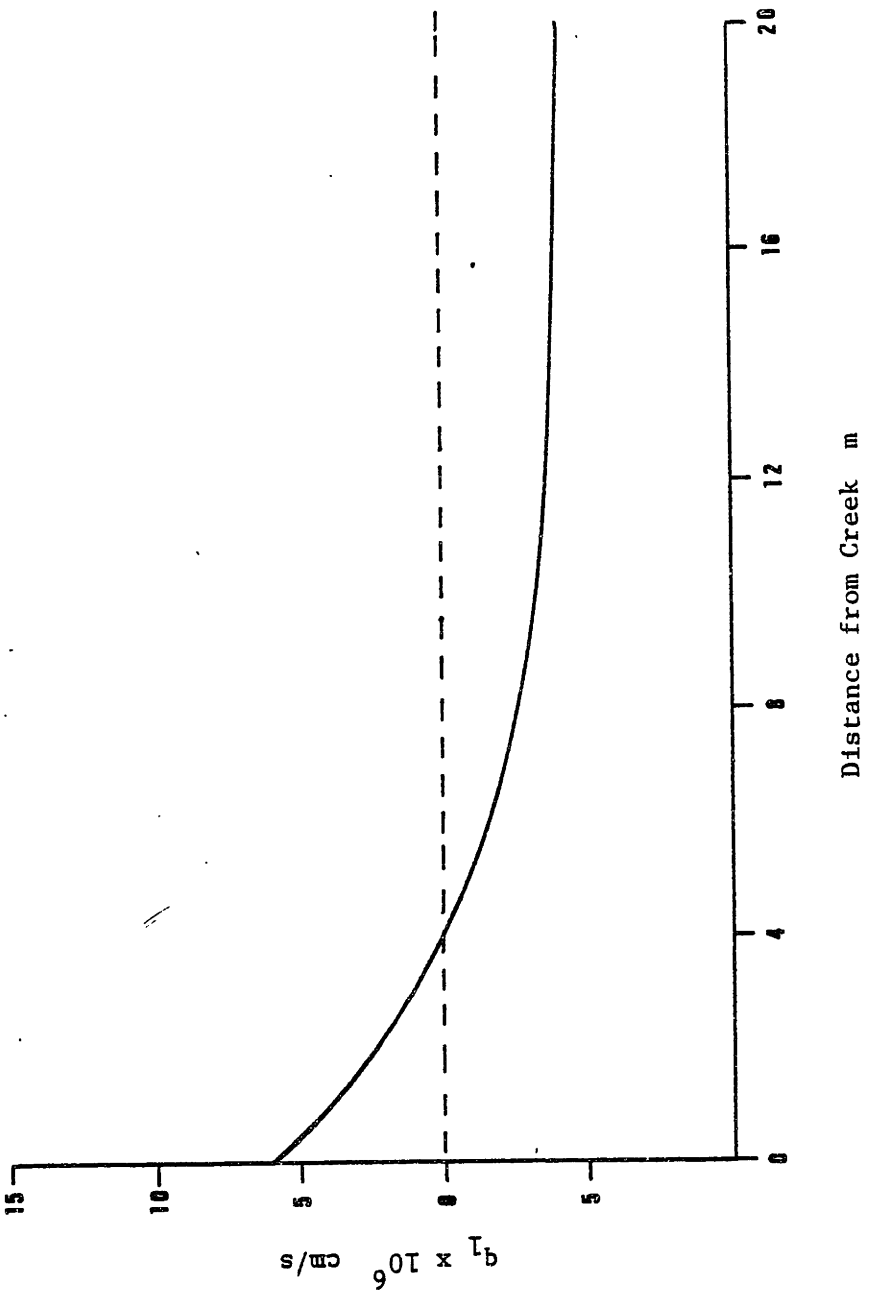

low, near zero. The steady state flow field possible during these seasons is simulated by case 6 by setting the evapotranspiration to zero.

Solutions for $\overline{\phi}(x)$ for the six cases described in table 4.3 are plotted in figure 4.10. The curves plotted here are equivalent to plots of the water table height in the peat. The general shape of these curves is suggestive of water table profiles observed by Gale (1980). The peak in the water table height observed in cases 3, 4, and 5 is present at the same location in some of the profiles observed by Gale (1980). The crest of a peak is the point at which the horizontal flow in the peat changes direction. On one side of the crest the flow is towards the creek; on the other side the flow is away from the creek.

Changes in the water balance in the peat are reflected in the profiles in figure 4.10. Close to the creek infiltration is high enough to balance the demand of evapotranspiration. The water table slopes sharply towards the creek in order to drain the excess infiltration and water upwelling from the sand aquifer. Away from the creek there is little infiltration, and evapotranspiration must be satisfied by upwelling fresh water. The flow is predominantly vertical in the peat away from the creek, so the horizontal gradient in the potential is small.

The rate of upwelling for several cases is shown in figure 4.11. The results of case 6 suggest that the direction of the steady exchange

Figure 4.10 Solutions for the Potential at Mid-Depth

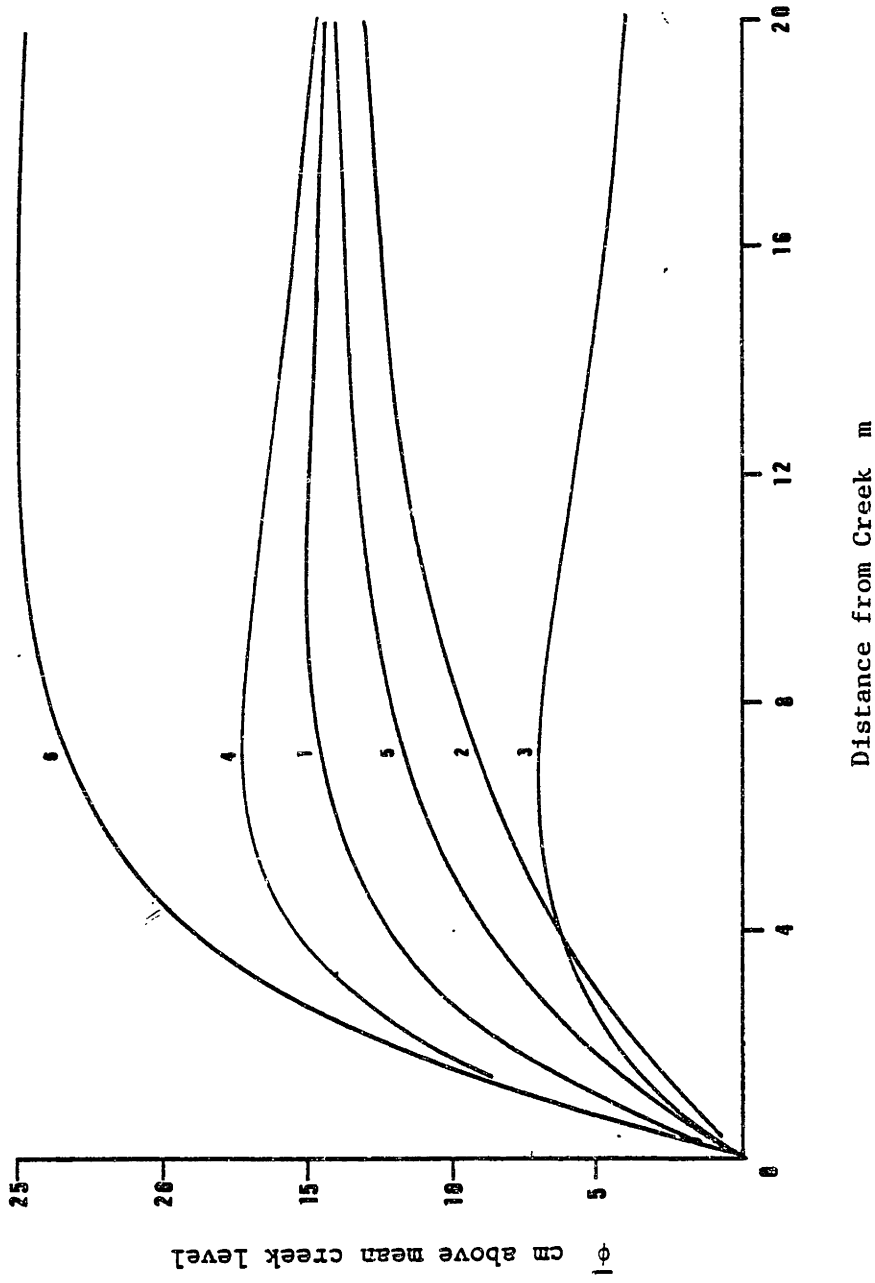

Figure 4.11 Fresh Water Input From the Sand Aquifer

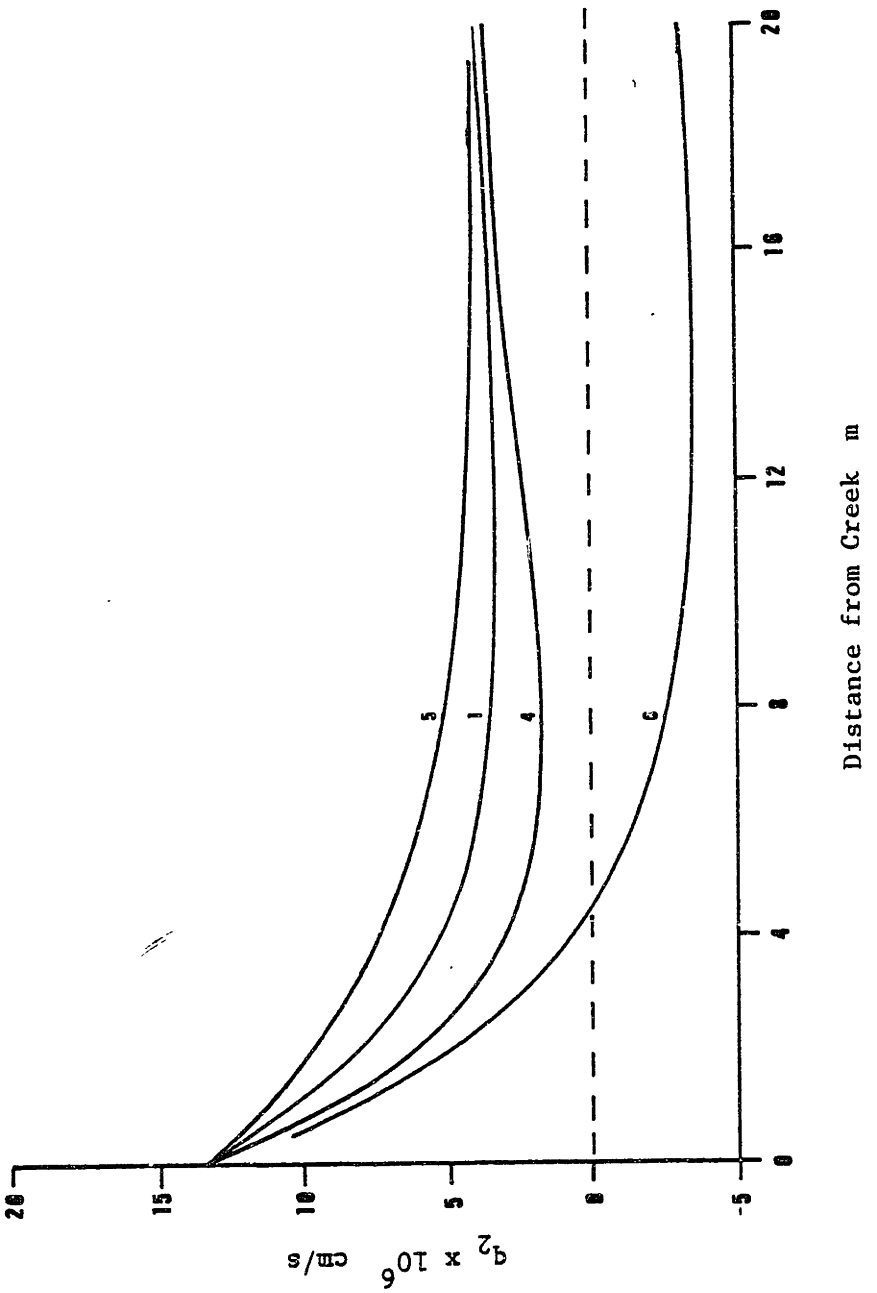

of water with the sand aquifer may reverse seasonally. The effect of seasonal changes in the average potential in the sand aquifer has not been considered. In all cases the strongest upwelling of fresh water occurs near the creeks.

Steady horizontal flow rates for several cases are tabulated in table 4.4. Exchange volumes across the creek bank due to the effect of tidal forcing were found to be on the order of 10 cm. Dividing by half the tidal period gives an average velocity of $\sim 4 \times 10^{-4}$ cm/s at the creek bank. The periodic velocity drops off exponentially as the distance from the creek bank increases. The average horizontal velocities due to tidal forcing at the creek are also tabulated in table 4.4. The periodic circulation in the peat dominates the flow in the first two meters from the creek. At ten meters the influence is negligible, and steady state processes control.

Table 4.4 Horizontal Velocities; $q_H \times 10^6$ cm/s

Distance From Creek cm	Steady State* 1	4	5	6	Tidal
10	110	150	70.5	163	372
100	81.0	106	55.8	123	195
200	57.0	70.2	43.1	89.0	95.0
300	39.0	44.9	33.3	64.1	46.7
400	26.0	27.0	25.7	45.8	22.8
500	17.0	15.0	19.9	32.4	11.1
1000	0.2	-5.2	5.5	4.3	0.3
2000	-0.9	-2.3	0.4	-0.6	-

* Positive flow when towards creek

5.0 Summary of Results

A study of water flow in salt marsh peat in the Great Sippewissett Marsh has been presented. Observations of the subsurface flow regime take two forms: 1) direct observations of water fluxes and piezometric potentials, and 2) laboratory determination of the hydraulic properties of peat. A simple linear flow equation has been derived from the basic principles of fluid flow in a saturated porous medium. Using this equation, some simple models of the flow patterns in the peat have been obtained. The models were tested by using the laboratory derived parameters to predict ranges of responses for the observed processes, without calibration. The comparison of model predictions and observations is good. Therefore, the flow models provide a means of describing the flow patterns in the peat. The flow of water in salt marsh peat was modeled for three processes: infiltration due to surface flooding, tidal forcing, and the long term water balance. The characteristics of the flow in each of these cases are summarized below.

5.1 Infiltration

A theory of infiltration into a saturated compressible soil was developed from consideration of the basic principles of fluid flow in a saturated medium in chapter 2. The volume of water that enters the peat when the peat surface is flooded by a high tide is a function of the hydraulic parameters of the peat (the hydraulic conductivity K and the compressive storativity $(1-n)\gamma_w a_v$), the pore pressure distribution in the peat prior to inundation, and the length of time

of inundation. The response of the piezometric potential during infiltration consists of two components: 1) the "static" component that responds to the increase in stress due to the depth of water flooding the peat surface, and 2) the "dynamic" response due to the reallocation of stress between the effective stress and pore pressure as water infiltrates into the peat. The volume of infiltration can be determined if the dynamic response of the potential is known.

The volume of infiltration can be approximated by an analytic expression involving the peat parameters, the initial pore pressure distribution, and the time since the beginning of inundation, equation 3.7. Using this expression, the distribution of peat parameters observed in the laboratory, and field conditions (pore pressures and periods of inundation) observed in the marsh, the observed range of infiltrated volumes is duplicated. The typical amount of infiltration occurring during an inundation of the marsh based on observation and model prediction ranges from 16 mm to less than 1 mm. Most events result in less than 5 mm of infiltration.

The dynamic component of the piezometric potential response to infiltration can be determined from direct piezometer readings by simply subtracting the depth of ponding on the surface. The dynamic potential response can also be approximated by an analytic model. In chapter 3 the theoretical dynamic potential response was fitted to the observed dynamic potential response to estimate the averaged peat parameters. This information was then used in the infiltration model to estimate the volume of infiltration responsible for the observed

piezometric potential response. This approach can be used as a general technique for measuring infiltration due to flooding. It has the advantage that although the volume of infiltration is small, on the order of millimeters, the quantity observed, the dynamic potential response, varies several centimeters. Direct measurement of infiltration volumes this small, for example the technique described by Hemond and Burke (1981), would require devices capable of measuring volume fluxes to millimeters.

5.2 Tidal Forcing

The boundary condition at the creek bank is a combination of a seepage face boundary above the creek level and an applied potential boundary below the creek level. The boundary condition is further complicated by the movement of the creek level in response to the tides. The response of the water in the peat to the dynamics of the creek bank boundary can be modeled in one dimension, vertically averaged. The vertically averaged creek bank boundary condition is not represented explicitly; however, any periodic function can, in principle, be represented by a Fourier series in which the contributions of many frequencies are represented as sinusoidal functions.

The response of the piezometric potential and the water fluxes in the peat due to a sinusoidal variation in potential at the creek bank is in both cases a sinusoidal function. The amplitude of the forced response in the peat decays exponentially with distance from the creek in a way that depends on the frequency of the forcing function and the peat parameters. Higher frequency forcing is

attenuated more quickly, and lower hydraulic conductivity attenuates more quickly. Periodic forcing at the period of the tides is fully attenuated 10 meters from the creek in most cases.

The creek bank boundary condition can be modeled to the first order by using only the component of the Fourier series corresponding to the tidal frequency. Higher frequency components can be neglected on the basis of lower amplitude and high attenuation in the peat. The volume of water exchanged across the creek bank is estimated to be on the order of 20 cm to 1.25 cm with volumes on the order of 10 cm or less most likely. Average flux rates across the creek bank in response to the tides are on the order of 4×10^{-4} cm/s. The effects of tidally induced potential variations in the underlying sand aquifer are less important due to lower amplitudes of variation and the presence of a low permeability layer of peat or clay at the interface. The response of water in the peat to components of the creek bank boundary condition with frequencies lower than the tidal frequency (storm surges, for example) can be similarly modeled if typical amplitudes are known.

5.3 Steady State Water Balance

The processes of precipitation and evapotranspiration in the marsh cannot yet be fully described, but estimates of long term (~ monthly) average fluxes across the peat surface due to these processes are available. Infiltration can be fairly well described in the short term, and is observed to vary in magnitude with distance from the creek due to the limiting effects of frequency of flooding

of the marsh surface. Estimates of the long term average flux across the surface of the peat have been made here in order to fully describe the water balance in the peat. The spatial variation of infiltration has been represented as an exponential function for convenience in the analysis. The steady state boundary conditions at the sand-peat interface and the creek bank are constant potential conditions determined by the time averaged components of the sand aquifer and creek bank potentials.

The water balance in the peat can be formulated in a manner similar to the approach used for leaky confined aquifers in groundwater hydraulics. Salt marsh peat has been observed to have a three layer structure in the Sippewissett Marsh, a permeable layer at mid-depth bounded by two less permeable layers. Horizontal flow in the peat occurs in the more permeable middle layer. Flow in the bounding layers is vertical, and these layers control the relation between the water balance in the middle layer and the upper and lower boundary conditions on the peat. By assuming some reasonable relations for the flow through the bounding layers in terms of the boundary conditions and conditions in the permeable layer, a solution for the flow in the permeable layer was obtained.

The horizontal flow of water in the peat towards the creek in the first one or two meters from the creek bank is dominated by the periodic exchange of water at the creek bank. Average periodic velocities are on the order of 10^{-4}cm/s to 4 x 10^{-4} cm/s in this region, and steady state velocities are on the order of 2 x 10^{-5} cm/s

to 1.5 x 10^{-4} cm/s. From three meters in from the creek to about eight meters the steady state velocities and periodic velocities are both of the same order of magnitude, 4 x 10^{-5} cm/s to 2 x 10^{-6} cm/s. The steady component may reverse direction and flow away from the creek at this point. The periodic velocities are fully damped out at ten meters from the creek and the horizontal flow in the peat becomes insignificant at about twenty meters.

Far from the creek the flow of water is generally vertically upward as fresh groundwater is drawn up to satisfy the demands of evapotranspiration (~ 7 x 10^{-6} cm/s). This flow may reverse direction seasonally in response to reduced evapotranspiration. There is a steady upwelling of fresh groundwater in the peat near the creek due to a difference between the average potential in the sand aquifer and on the creek bank. Groundwater upwelling into the peat near the creek bank contributes to the horizontal flow towards the creek. Between the creek bank region and the interior region, the rate of upward groundwater flow may reach a minimum. Here evapotranspiration is more nearly balanced by infiltration and precipitation and the low conductivity of the peat and the distance to the creek inhibit horizontal drainage to the creek.

The dynamic flow patterns that occur within the peat as a result of the time dependence of the processes acting at the surface boundary of the peat have not been considered in this analysis. More information is needed on the rates associated with the processes of evapotranspiration and precipitation and their distribution in time. Instantaneous

fluxes due to infiltration, evapotranspiration, and precipitation are likely to be orders of magnitude larger than their long term averages and could temporarily reverse the long term flow patterns deduced from the steady state water balance.

REFERENCES

Bear, J. 1972. Dynamics of Fluids in Porous Media. American Elsevier. New York.

_____. 1979. Hydraulics of Groundwater. McGraw Hill. New York.

Burke, R. 1979. Infiltration in a New England Salt Marsh. Master's Thesis. Massachusetts Institute of Technology.

Burke, R.W., H.F. Hemond, and K.D. Stolzenbach. Surface Infiltration in Two Massachusetts Salt Marshes. Unpublished. 8 p.

Carslaw, H.S., and J.C. Jaeger. 1959. Conduction of Heat in Solids. Oxford University Press.

Climatological Data Annual Summary; New England. 1978. National Oceanic and Atmospheric Administration. 90(13).

Earth Manual. 1968. U.S. Department of Interior. Bureau of Reclamation. 1st Ed. 541 p.

Fifield, J.L. 1981. Peat Hydrology in Two New England Salt Marshes: A Field and Model Study. Master's Thesis. Massachusetts Institute of Technology.

Freeze, R.A. 1975. A Stochastic-Conceptual Analysis of One-Dimensional Groundwater Flow in Nonuniform Homogeneous Media. Water Resources Research. 11(5):725-741.

Freeze, R.A., and J.A. Cherry. 1979. Groundwater. Prentice-Hall, Inc. Englewood Cliffs, New Jersey.

Gale, J.A. 1980. Observations on Infiltration, Permeability, Peat Water Content and Water Table Height at Great Sippewissett Marsh. Report. Ecosystems Center, Marine Biological Laboratory. Woods Hole, Massachusetts.

Gardner, L.R. 1973. The Effect of Hydrologic Factors on Pore Water Chemistry of Intertidal Marsh Sediments. Southeast Geology. 15:17-28.

Hemond, H.F. 1982. A Low-Cost Multichannel Recording Piezometer System for Wetland Research. Water Resources Research. 18(1):182-186.

Hemond, H.F., and R. Burke. 1981. A Device for the Measurement of Infiltration in Intermittenly Flooded Wetlands. Limnology and Oceanography. 27(1):126-136.

Hemond, H.F., and J.L. Fifield. 1982. Subsurface Flow in Salt Marsh Peat: A Model and Field Study. Limnology and Oceanography. 27(1):126-136.

Howarth, R.W., and J.M. Teal. 1979. Sulfate Reduction in a New England Salt Marsh. Limnology and Oceanography. 24(6):999-1013.

Howland, M.D. 1976. Hydrogeology of the Palo Alto Baylands, Palo Alto, California with Emphasis on the Tidal Marshes. Masters Thesis. Stanford University. 138 p.

Lambe, W.T. 1951. Soil Testing for Engineers. John Wiley and Sons. New York.

Lambe W.T., and R.V. Whitman. 1969. Soil Mechanics. John Wiley and Sons. New York.

Lee, D.R. 1977. A Device for Measuring Seepage Flux in Lakes and Estuaries. Limnology and Oceanography. 22(1):140-147.

Lindberg, S.E., and R.C. Harriss. 1973. Mechanisms Controlling Pore Water Salinities in a Salt Marsh. Limnology and Oceanography. 18:788-791.

Narasimhan, T.N. 1979. The Significance of the Storage Parameter in Saturated-Unsaturated Groundwater Flow. Water Resources Research. 15(3):569-576.

Niedorada, A., and R. April. 1975. Report on Groundwater Flow Beneath Coastal Salt Marshes. Submitted to National Park Service Cooperative Studies at the University of Massachusetts. 49 p.

Redfield, A.C. 1972. Development of a New England Salt Marsh. Ecological Monographs. 42(2):201-237.

Teal, J.M., and J.W. Kanwisher. 1970. Total Energy Balance in Salt Marsh Grasses. Ecology. 51(4):690-695.

Appendix: Derivation of the Flow Equations and Some Solutions

A1.0 Linearization of the Basic Equations of Flow

A2.0 Solutions in One Dimension

A) Step Change in Potential: Semi-Infinite Solution

B) Fluid Flux Due to a Step Change in Potential

C) Sinusoidal Boundary Potential

D) Fluid Flux Due to a Sinusoidal Boundary Potential

E) Solutions with a Boundary Condition at X=L

A3.0 Solution to the Steady State Water Balance Equation

A1.0 LINEARIZATION OF THE BASIC EQUATIONS OF FLOW

The basic relation for fluid flow through a porous medium is Darcy's Law which states that the discharge per unit area in proportional to the gradient in the piezometric head of the fluid.

$$q = -K \frac{\partial \phi}{\partial x} \qquad [1]$$

The constant of proportionality K is known as the hydraulic conductivity and is known to depend on the properties of the fluid and the porous medium. The piezometric head at a point ϕ is defined as

$$\phi = z_o + \int_{p_o}^{p} \frac{dp}{\gamma(p)} \qquad [2]$$

for compressible fluids, where Z_o is the distance from an arbitrary datum at which the pressure in the fluid is P_o. Darcy's Law can be generalized to three dimensions with the result in index notation being

$$q_i = -K_{ij} \frac{\partial \phi}{\partial x_j} \qquad [3]$$

In addition to the dependence on material and fluid properties mentioned above, the hydraulic conductivity is in general also a function of location, piezometric head, and time. Piezometric head is a function of location and time.

Darcy's Law in three dimensions gives three equations in four unknowns, x, y, z, and t. A fourth relation is needed in order to solve for the flow field, the principle of mass conservation. Consider the fluid mass balance on the volume of porous material enclosed by surface S shown in figure A1. The rate of change of M_v, the fluid mass content per unit volume of

Figure A1

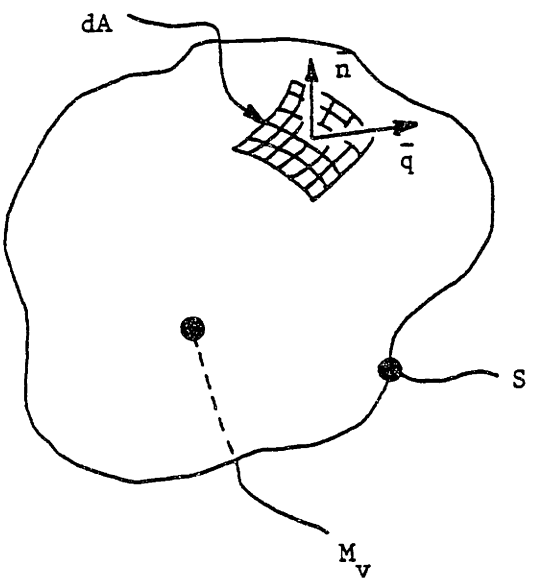

porous material, due to the balance between the influx and efflux of mass across the surface S is given by:

$$\int_v \frac{\partial}{\partial t} M_v \, dV = -\int_s \rho q_i n_i \, dA \qquad [4]$$

where ρ is the fluid density and n_i is the outward unit normal to area dA. Substituting for q_i from [3] and invoking Gauss's Theorem results in

$$\int_v \frac{\partial}{\partial t} M_v \, dV = \int_v \frac{\partial}{\partial x_i} (\rho K_{ij} \frac{\partial \phi}{\partial x_j}) dV \qquad [5]$$

from which it can be deduced that

$$\frac{\partial}{\partial t} M_v = \frac{\partial}{\partial x_i} (\rho K_{ij} \frac{\partial \phi}{\partial x_j}) \qquad [6]$$

This is the statement of conservation of mass at a point for flow through a porous medium. The quantity M_v, the fluid mass content, is defined mathematically at a point but must be treated as an average over some representative elementary volume of material. The fluid mass content is defined by

$$M_v = \rho n S \qquad [7]$$

where n is the porosity of the porous material, defined as the ratio of the void volume to the total volume of the material, and S is the degree of saturation, the ratio of the volume of fluid to the volume of voids. From [7] it follows that

$$\frac{\partial}{\partial t} M_v = nS \frac{\partial \rho}{\partial t} + \rho S \frac{\partial n}{\partial t} + \rho n \frac{\partial S}{\partial t} \qquad [8]$$

It can be seen that the change in the fluid mass content is the result of three processes corresponding to the three terms on the right-hand-side of equation [8]; compression of the fluid, change in the void ratio of the porous material, and saturation-desaturation of the void spaces. The effects of fluid compressibility and saturation-desaturation are neglected in this analysis; full saturation is assumed. It is further

assumed that the change in porosity, the result of compression of the porous material, occurs in such a way that the volume of the solid phase remains constant. It is convenient now to introduce a new parameter e the void ratio equal to the volume of the void space divided by the volume of the solid phase. Porosity and the void ratio are related as below.

$$n = (1-n)e \qquad [9]$$

where it can be seen that (1-n) is the volume of the solid phase per unit volume of material.

The void ratio can be expressed in terms of a third parameter, the effective stress σ'. The effective stress at a point is defined in terms of the total stress σ_T and the fluid pressure p by

$$\sigma_T = \sigma' + p \qquad [10]$$

The piezometric head ϕ defined in [2] simplifies for the case of an incompressible fluid (this assumption is made above) to

$$\phi = z_o + \frac{p}{\gamma_w} \qquad [11]$$

from which it follows that

$$\sigma' = \sigma_T - \gamma_w(\phi - z_o) \qquad [12]$$

If it is assumed that the total stress at a point σ_T is constant and that changes in Z_o due to the compression of the material can be neglected then

$$d\sigma' = -d(\gamma_w \phi) \qquad [13]$$

The function $e(\sigma')$ can be determined experimentally for a given material. The most common form of this relationship, the one that generally best fits the data, is

$$e = A \log_{10} \sigma' + B \qquad [14]$$

$$\frac{de}{d\sigma'} = A/2.303\sigma'$$

where A is called the compression index and is usually denoted as C_c. This relationship has the disadvantage of retaining the independent variable σ' in the analysis. To avoid this a linear relation for $e(\sigma')$ can be used.

$$e = A\sigma' + B \qquad [15]$$

$$\frac{de}{d\sigma'} = A$$

Here A is known as the coefficient of compressibility and is usually denoted as a_v.

Now, from the conservation of fluid mass relation [6] and equations [8], [9], [13], and [15] and the assumptions of incompressible fluid and total saturation, a revised conservation equation is obtained.

$$\rho S(1-n)\gamma_w a_v \frac{\partial \phi}{\partial t} = \frac{\partial}{\partial x_i}\left(\rho K_{ij}\frac{\partial \phi}{\partial x_j}\right) \qquad [16]$$

If the hydraulic conductivity is assumed constant and isotropic, then the linearized conservation of mass equation is obtained.

$$\frac{\partial \phi}{\partial t} = \alpha \frac{\partial^2 \phi}{\partial x_i^2} \qquad [17]$$

$$\alpha = \frac{K}{(1-n)\gamma_w a_v}$$

in which S=1.0 for fully saturated conditions has been used. Notice that α has dimensions $[L^2/T]$.

The linearized mass conservation relation [17] has the familiar form of a heat diffusion equation and is amenable to analytic solution. It will be helpful to keep in mind whenever this formulation is used that the following assumptions were necessary in order to derive the linearized relation:

1) incompressible fluid;

2) fully saturated porous medium, S=1;

3) constant volume of the solid phase;

4) constant total stress at a point;

5) negligible change in elevation of a point due to the compression of the porous material;

6) void ratio linearly related to effective stress with constant of proportionality a_v;

7) constant hydraulic conductivity; and

8) isotropic hydraulic conductivity.

A2.0 SOLUTIONS IN ONE DIMENSION

The mass conservation equations [17] reduces to the following form in one dimension

$$\frac{\partial \phi}{\partial t} = \alpha \frac{\partial^2 \phi}{\partial x^2} \qquad [18]$$

Solutions for this differential equation with various boundary conditions will be derived in this section.

A) STEP CHANGE IN POTENTIAL - SEMI-INFINITE SOLUTION

The initial and boundary conditions on (x,t) for a step change on the boundary of a half plane are:

$$\begin{aligned} &1)\ \phi(x,0) = 0 && x > 0 \\ &2)\ \phi(0,t) = \phi_o && t > 0 \\ &3)\ |\phi(x,t)| < \infty && t > 0;\quad 0 < x \leq \infty \end{aligned} \qquad [19]$$

The third condition is the requirement that the solution be finite valued everywhere in the half plane. The solution obtained by application of Laplace transforms is

$$\phi(x,t) = \phi_o \mathrm{ERFC}\left(\frac{x}{\sqrt{4\alpha t}} \right) \qquad x > 0;\quad t > 0 \qquad [20]$$

where ERFC(z) is the complementary error function and is defined by

$$\mathrm{ERFC}(z) = 1 - \frac{2}{\sqrt{\pi}} \int_0^z e^{-t^2} dt \qquad [21]$$

B) FLUID FLUX DUE TO A STEP CHANGE IN POTENTIAL

The transient fluid flux response can be obtained by application of Darcy's Law and the solution for $\phi(x,t)$ obtained above.

$$q(x,t) = \frac{K\phi_o}{\sqrt{\pi \alpha t}} \mathrm{EXP}\left(\frac{-x^2}{4\alpha t} \right) \qquad x > 0;\quad t > 0 \qquad [22]$$

where the relation

$$\frac{d}{dx}\,\mathrm{ERFC}(z) = \frac{-2}{\sqrt{\pi}}\, e^{-z^2}\frac{dz}{dx} \qquad [23]$$

has been used.

C) SINUSOIDAL VARIATION OF POTENTIAL WITH TIME

The intial and boundary conditions for the case of a sinusoidal variation in potential on the surface of a half plane are:

$$\begin{aligned} &1)\quad \phi(x,0) = \phi_o && x > 0 \\ &2)\quad \phi(0,t) = \phi_o \cos \omega t && t > 0 \\ &3)\quad |\phi(x,t)| < \infty && t > 0;\quad 0 < x < \infty \end{aligned} \qquad [24]$$

The solution is presented by Carslaw and Jaeger.

$$\phi(x,t) = \phi_o \mathrm{EXP}\left(-\sqrt{\frac{\omega}{2\alpha}}\, x \right) \cos\left(\omega t - \sqrt{\frac{\omega}{2\alpha}}\, x + \varepsilon \right) + \qquad [25]$$

$$-\phi_o \frac{2}{\sqrt{\pi}} \int_0^{\frac{x}{\sqrt{4\alpha t}}} \cos\left\{ \omega\left(t - \frac{x^2}{4\alpha u^2}\right)\right\} e^{-u} du$$

The first term on the right hand side represents the steady state solution. The second term is the transient response due to the initial conditions imposed in [24]. The solution to the case of sinusoidal forcing is interesting only as an analog to tidal forcing so only the steady state term is desired. Therefore, the solution of interest is

$$\phi(x,t) = \phi_o \mathrm{EXP}\left(-\sqrt{\frac{\omega}{2\alpha}}\, x \right) \cos\left(\omega t - \sqrt{\frac{\omega}{2\alpha}}\, x + \varepsilon \right) \qquad [26]$$

where ε is an arbitrary phase angle.

D) FLUID FLUX IN RESPONSE TO A SINUSOIDAL VARIATION IN POTENTIAL.

The fluid flux at any point in the half plane due to sinusoidal variation of the potential on its surface is obtained by Darcy's Law.

$$q(x,t) = K\phi_o\sqrt{\frac{\omega}{\alpha}}\ \mathrm{EXP}\left(-\sqrt{\frac{\omega}{2\alpha}}\ x \right) \cos\left(\omega t - \sqrt{\frac{\omega}{2\alpha}}\ x + \frac{\pi}{4} + \varepsilon \right) \quad [27]$$

E) SOLUTIONS WITH A BOUNDARY CONDITION AT X=L

The solutions derived so far have been for the semi-infinite problem ($0<x<\infty$). The method of images can be used to derive solutions when a boundary condition is imposed at X=L. The method of images solution for the case of a constant potential $\phi(x,t)= 0$ imposed at X=L is

$$\phi(x,t) = \phi_i(x,t) - \phi_i(2L - x,t) \quad 0 < x < L; \quad t > 0 \quad [28]$$

where $\phi_i(x,t)$ is the solution of the semi-infinite problem for the corresponding initial and boundary condition imposed at X=0. The method of images solution for the case of an impermeable boundary ($\frac{\partial}{\partial x}\phi(x,t) = 0$) at X=L is

$$\phi(x,t) = \phi_i(x,t) + \phi_i(2L - x,t) \quad 0 < x < L; \quad t > 0 \quad [29]$$

A3.0 SOLUTION TO THE STEADY STATE WATER BALANCE EQUATION

The following linear differential equation is obtained from the consideration of the horizontal water balance in salt marsh peat,

$$\frac{d^2\bar{\phi}}{dx^2} - \frac{B}{A}\bar{\phi} = \frac{C}{A} + \frac{D}{A} e^{-\gamma x} \qquad [30]$$

The boundary conditions are

$$\begin{aligned} &1) \quad \bar{\phi}(0) = 0 \\ &2) \quad \frac{d\bar{\phi}}{dx} \to 0 \qquad x \to \infty \end{aligned} \qquad [31]$$

The solution for $\bar{\phi}(x)$ will be obtained as the sum of the solution to the homogeneous equation and the solutions of two non-homogeneous equations.

The homogeneous equation

$$\frac{d^2\bar{\phi}}{dx^2} - \frac{B}{A}\bar{\phi} = 0 \qquad [32]$$

has the general solution

$$\bar{\phi}_H = S_1 e^{-\sqrt{xB/A}} + S_2 e^{\sqrt{xB/A}} \qquad [33]$$

A solution to the non-homogeneous problem

$$\frac{d^2\phi}{dx^2} - \frac{B}{A}\bar{\phi} = \frac{C}{A} \qquad [34]$$

is

$$\bar{\phi}_1 = -\frac{C}{B} \qquad [35]$$

A solution to the non-homogeneous problem

$$\frac{d^2\bar{\phi}}{dx^2} - \frac{B}{A}\bar{\phi} = \frac{D}{A} e^{-\gamma x} \qquad [36]$$

is

$$\bar{\phi}_2 = \frac{D/A}{(\gamma^2 - B/A)} e^{-\gamma x} \qquad [37]$$

The general solution to equation 30 is the sum of equations 33, 35, and 37.

$$\bar{\phi}(x) = S_1 e^{-\sqrt{xB/A}} + S_2 e^{\sqrt{xB/A}} + \frac{D/A}{(\gamma^2 - B/A)} e^{-\gamma x} - \frac{C}{B} \qquad [38]$$

The coefficients S_1 and S_2 are evaluated using the boundary condition equations 31 , to obtain the final form of the solution.

$$\bar{\phi}(x) = \left[\frac{C}{B} - \frac{D/A}{(\gamma^2 - B/A)}\right] e^{-\sqrt{xB/A}} + \frac{D/A}{(\gamma^2 - B/A)} e^{-\gamma x} - \frac{C}{B} \quad [39]$$